Equivalent multipolar point-source modeling of small spheres for fast and accurate electromagnetic wave scattering computations

Justine Labat, Victor Péron, Sébastien Tordeux

Equivalent multipolar point-source modeling of small spheres for fast and accurate electromagnetic wave scattering computations

Justine Labat[a,*], Victor Péron[a], Sébastien Tordeux[a]

[a]*EPC Magique 3D - University of Pau and Pays de l'Adour, E2S-UPPA, LMAP UMR CNRS 5142, INRIA Bordeaux Sud-Ouest - Avenue de l'Université, 64000 Pau, France*

Abstract

In this paper, we develop reduced models to approximate the solution of the electromagnetic scattering problem in an unbounded domain which contains a small perfectly conducting sphere. Our approach is based on the method of matched asymptotic expansions. This method consists in defining an approximate solution using multi-scale expansions over outer and inner fields related in a matching area. We make explicit the asymptotics up to the second order of approximation for the inner expansion and up to the fifth order for the outer expansion. We validate the results with numerical experiments which illustrate theoretical orders of convergence for the asymptotic models requiring negligible computational cost.

Keywords: Matched asymptotic expansions, Maxwell's equations, Reduced models, Scattering by spheres, Multipoles

1. Introduction

Many physical phenomena involve multiple electromagnetic scattering by obstacles whose the characteristic size is very small in comparison with the wavelength [1, 2, 3, 4]. All exact theories and numerical techniques for computing the electromagnetic fields are based on the resolution of the Maxwell's equations. Numerical simulation of scattering by small obstacles using finite difference or finite element methods can become very expensive or not affordable in terms of computational time and memory capacity even in the context of mesh refinement and parallel computation. Methods based on boundary integral equations can be very efficient in solving multiple scattering problems [5, 6, 7] compared to volumical methods. In low-frequency regime, boundary element methods involve dense matrices with a large number of degrees of freedom due to a thin surface discretization. Spectral-based boundary element methods [8, 9, 10, 11] take advantage of the good properties of mesh-less methods. These methods can be expressed analytically when geometry admits a coordinate system in which the equation is separable. In the context of single scattering by a sphere, the induced model will correspond to the Mie theory.

*Corresponding author

Email addresses: justine.labat@inria.fr (Justine Labat), victor.peron@inria.fr (Victor Péron), sebastien.tordeux@inria.fr (Sébastien Tordeux)

The multiscale asymptotic analysis of problems posed in singularly perturbed domains, such as domains with small holes, has turned out to be very efficient to define reduced models adapted to low cost numerical techniques. Indeed, it enables to consider the size of the obstacle as a parameter which does not act from a geometrical point of view [12, 13, 14, 15]. The resulting approaches provide algorithms to compute approximate solutions at any order with respect to the small parameter [8, 16, 17, 18, 19]. The method of matched asymptotic expansions, which brought out of this branch of analysis, consists in defining local approximations of the solution in different regions of the domain of propagation with appropriate scales, and matching them in an intermediate area [14, 20, 21]. The justification of matching rules is obtained thanks to the introduction of a uniformly valid expansion in the whole domain [22]. Typically, this method is used for the single scattering case and the extension to multiple scattering is done with suitable models relying on Born or Foldy-Lax theory for instance, see [23, 24, 25, 26].

Problems dealing with electromagnetic scattering by small obstacles have given rise to numerous works. In [8], Ammari *et al.* derived high-order asymptotics for coated spheres which are used in order to enhance near-cloaking of electromagnetic waves. In [19], Korikov and Plamenevskii used the method of multi-scale expansions to approximate the solution of the interior Maxwell problem with a small hole, both for time-harmonic and time-dependent Maxwell equations. They set up a rigorous framework to express asymptotic expansions, including elliptic regularization, at any order. Error estimates are performed for dissipative equations. In [27], Ammari and Khelifi derived second order asymptotic expansions for the single scattering problem by small dielectric inhomogeneities. In [28], asymptotic formulas for perturbations in tangential trace of the magnetic field caused in the presence of heterogeneities are derived and rigorously justified. These formulas are used in the theory of inverse problems through boundary integral methods in order to determine physical properties, localization and size of the obstacles [29, 30]. In [25], the Foldy-Lax model is used to solve direct and inverse time-harmonic electromagnetic scattering problems for a finite number of isotropic point-like obstacles in three dimensions and in [24] for small conductive bodies of arbitrary shape. In particular, consideration of obstacles of arbitrary shape involves the introduction of polarization tensors [31, 32].

In this paper, we apply the method of matched asymptotic expansions to approximate the solution of the time-harmonic Maxwell problem into an unbounded domain which contains a small perfectly conducting spherical obstacle. This method leads to a collection of elementary problems that can be solved analytically in spherical geometries. For a spherical obstacle, we derive explicitly the first terms of the asymptotics, up to the second order for the inner expansion and up to the fifth order for the outer expansion. Moreover, we give a physical interpretation of the first terms through the idealistic notion of electromagnetic multipoles. These new results are illustrated and validated with numerical simulations. These expansions can be retrieved by considering Taylor expansions of the Mie series expansions associated with the exterior Maxwell problem [33, Sections C.3.3 and D.2]. This expression is more complex to obtain than the one of Mie theory due to the definition of two different expansions related through a matching procedure. However, it allows finally to get simpler expressions of the approximations than the truncated Mie series expansions. Furthermore, these approximations are valid for any incident field and the numerical treatment does not require neither computation of the vector spherical harmonics nor exact computation or numerical approximation of spectral coeffcients associated with the incident fields. The extension to obstacles of arbitrary shape appears to be more feasible than with Mie series.

This article is organized as follows. In Section 2, we describe the time-harmonic electromagnetic scattering problem and we introduce the main results. The first terms of the asymptotic expansions are analytically derived using the technique of separation of variables on the elementary problems provided by the matched asymptotic expansions method, see also Appendix A. In Sections 3 then 4, we introduce some applications of the asymptotics. We show how the obstacle can be replaced by equivalent multipolar point-sources. Then, we define a collected dipolar model relying on the physical interpretation and an extension to multiple scattering problem based on a superposition principle. In Section 5, we present some numerical results which illustrate the performance of the asymptotic models by considering two different incident waves. Finally, we provide in Section 6 our conclusion and we describe some of the perspective of our work.

2. Problem description and main result

2.1. Description of scattering problem

The propagation of time-harmonic electromagnetic waves of angular frequency $\omega > 0$ in a homogeneous, isotropic and linear dielectric medium with electric permittivity $\varepsilon > 0$ and magnetic permeability $\mu > 0$ is described by incident electromagnetic fields,

$$\begin{cases} \boldsymbol{\mathcal{E}}^{\mathrm{i}}(x,t) = \Re\left[\varepsilon^{-\frac{1}{2}}\boldsymbol{E}^{\mathrm{i}}(x)\exp(-i\omega t)\right], & x \in \mathbb{R}^3, \quad t > 0, \\ \boldsymbol{\mathcal{H}}^{\mathrm{i}}(x,t) = \Re\left[\mu^{-\frac{1}{2}}\boldsymbol{H}^{\mathrm{i}}(x)\exp(-i\omega t)\right], & x \in \mathbb{R}^3, \quad t > 0, \end{cases}$$

where the corresponding phasors $(\boldsymbol{E}^{\mathrm{i}}, \boldsymbol{H}^{\mathrm{i}})$ satisfy the reduced Maxwell equations in the free-space

$$\begin{cases} \nabla \times \boldsymbol{E}^{\mathrm{i}} - i\kappa\boldsymbol{H}^{\mathrm{i}} = 0 & \text{in } \mathbb{R}^3, \\ \nabla \times \boldsymbol{H}^{\mathrm{i}} + i\kappa\boldsymbol{E}^{\mathrm{i}} = \dfrac{\mathbf{j}}{c} & \text{in } \mathbb{R}^3. \end{cases}$$

We assume that the electric current density $\mathbf{j}$ is a smooth vector field with compact support in $\mathbb{R}^3$. The wave-number κ satisfies the dispersion relation

$$\kappa = \frac{\omega}{c}$$

with the wave-speed $c = (\mu\varepsilon)^{-\frac{1}{2}}$. In the presence of a small obstacle with characteristic length δ, the incident field $(\boldsymbol{E}^{\mathrm{i}}, \boldsymbol{H}^{\mathrm{i}})$ is scattered and gives birth to outgoing electromagnetic fields $(\boldsymbol{E}_\delta, \boldsymbol{H}_\delta)$ solving the time-harmonic Maxwell equations. These scattered fields strongly depend on the geometry and the physical properties of the obstacle. In this paper, we consider the electromagnetic scattering problem by a single perfectly conducting sphere $\mathcal{B}(0,\delta)$ centered at the origin with small radius $\delta > 0$ such that $\kappa\delta \ll 1$, see Figure 1. The domain of propagation Ω_δ is the exterior domain defined by

$$\Omega_\delta = \mathbb{R}^3 \setminus \overline{\mathcal{B}(0,\delta)}.$$

Then, the scattering problem reads as

$$\begin{cases} \nabla \times \boldsymbol{E}_\delta - i\kappa\boldsymbol{H}_\delta = 0 & \text{in } \Omega_\delta, \\ \nabla \times \boldsymbol{H}_\delta + i\kappa\boldsymbol{E}_\delta = 0 & \text{in } \Omega_\delta, \\ \mathbf{n} \times \boldsymbol{E}_\delta = -\mathbf{n} \times \boldsymbol{E}^{\mathrm{i}} & \text{on } \partial\Omega_\delta, \\ \mathbf{n} \cdot \boldsymbol{H}_\delta = -\mathbf{n} \cdot \boldsymbol{H}^{\mathrm{i}} & \text{on } \partial\Omega_\delta, \\ \lim\limits_{r\to\infty} r(\boldsymbol{H}_\delta \times \widehat{x} - \boldsymbol{E}_\delta) = 0 & \text{uniformly in } \widehat{x} = \dfrac{x}{r}, \end{cases} \tag{2.1}$$

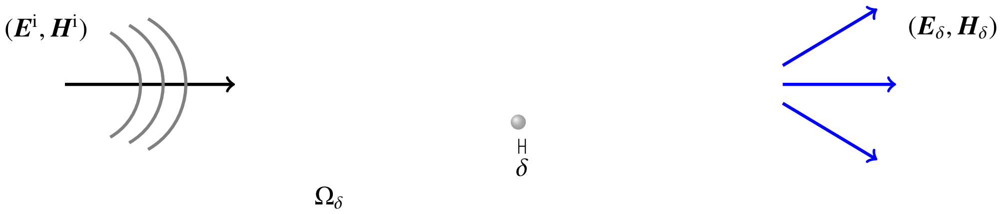

Figure 1: Domain of propagation

where $r = |x|$ and $\mathbf{n}$ denotes the inward-pointing normal unit vector of Ω_δ. It is well-known that the electromagnetic scattering problem by a single sphere is well-posed in $\mathbf{H}_{\mathrm{loc}}(\nabla\times, \Omega_\delta)$, see for instance [34, 35, 36]. In the sequel, for any smooth vector field $\boldsymbol{u}$, we denote by $\gamma_{\mathrm{n}}[\boldsymbol{u}]$, $\gamma_{\mathrm{t}}[\boldsymbol{u}]$ and $\gamma_\times[\boldsymbol{u}]$ its radial and tangential traces relatively to the sphere, defined for $x = r\widehat{x} \in \mathbb{R}^3$ by

$$\gamma_{\mathrm{n}}[\boldsymbol{u}](x) = \widehat{x} \cdot \boldsymbol{u}(\widehat{x}), \qquad \gamma_{\mathrm{t}}[\boldsymbol{u}](x) = \boldsymbol{u}(\widehat{x}) - \gamma_{\mathrm{n}}[\boldsymbol{u}](x)\,\widehat{x}, \qquad \gamma_\times[\boldsymbol{u}](x) = \widehat{x} \times \gamma_{\mathrm{t}}[\boldsymbol{u}](x). \tag{2.2}$$

Remark 1. The scalar field $\gamma_{\mathrm{n}}[\boldsymbol{u}]$ and the vector fields $\gamma_{\mathrm{t}}[\boldsymbol{u}]$ and $\gamma_\times[\boldsymbol{u}]$ will depend on $\widehat{x}$ even if the vector field $\boldsymbol{u}$ is constant. In the rest of the paper, we will denote $\gamma_\diamond[\boldsymbol{u}](x)$ and $\gamma_\diamond[\boldsymbol{u}]$ indifferently, for $\diamond = \mathrm{n}$, t or $\times$.

2.2. *Asymptotic expansions*

In this paragraph, we introduce the outer and inner approximations of the solution to problem (2.1), up to fifth order for the outer expansion and up to second order for the inner expansion. These formulas have been obtained in Appendix A thanks to the method of matched asymptotic expansions. Outside the immediate vicinity of the small scatterer, the exact solution $(\boldsymbol{E}_\delta, \boldsymbol{H}_\delta)$ possesses the following formal asymptotic expansion

$$\boldsymbol{E}_\delta = \delta^3 \widetilde{\boldsymbol{E}}_3 + \delta^5 \widetilde{\boldsymbol{E}}_5 + \ldots, \qquad\qquad \boldsymbol{H}_\delta = \delta^3 \widetilde{\boldsymbol{H}}_3 + \delta^5 \widetilde{\boldsymbol{H}}_5 + \ldots.$$

For any $x \in \Omega^\star = \mathbb{R}^3 \setminus \{0\}$, the third-order outer terms $\widetilde{\boldsymbol{E}}_3$ and $\widetilde{\boldsymbol{H}}_3$ are given by

$$\begin{aligned}
\widetilde{\boldsymbol{E}}_3(x) &= -\frac{\kappa^3}{2} h_1^{(1)}(\kappa r)\gamma_\times[\boldsymbol{H}^{\mathrm{i}}(0)] - \kappa^3 \widetilde{h}_1^{(1)}(\kappa r)\gamma_{\mathrm{t}}[\boldsymbol{E}^{\mathrm{i}}(0)] - 2\kappa^3 \frac{h_1^{(1)}(\kappa r)}{i\kappa r}\gamma_{\mathrm{n}}[\boldsymbol{E}^{\mathrm{i}}(0)]\,\widehat{x}, \\
\widetilde{\boldsymbol{H}}_3(x) &= -\kappa^3 h_1^{(1)}(\kappa r)\gamma_\times[\boldsymbol{E}^{\mathrm{i}}(0)] + \frac{\kappa^3}{2} \widetilde{h}_1^{(1)}(\kappa r)\gamma_{\mathrm{t}}[\boldsymbol{H}^{\mathrm{i}}(0)] + \kappa^3 \frac{h_1^{(1)}(\kappa r)}{i\kappa r}\gamma_{\mathrm{n}}[\boldsymbol{H}^{\mathrm{i}}(0)]\,\widehat{x},
\end{aligned} \tag{2.3}$$

where γ_{n}, γ_{t} and $\gamma_\times$ are defined by (2.2), see also Remark 1. For any non-negative integer n, $h_n^{(1)}$ is the spherical Hankel function of first kind of order n, see for instance [37], and $\widetilde{h}_n^{(1)}$ is given by

$$\widetilde{h}_n^{(1)}(z) = \frac{h_n^{(1)}(z)}{iz} - i\frac{d}{dz}\left[h_n^{(1)}(z)\right], \qquad \text{with} \qquad h_n^{(1)}(z) = -iz^n \left[-\frac{1}{z}\frac{d}{dz}\right]^n \frac{\exp(iz)}{z}.$$

Furthermore, for any $x \in \Omega_\delta$, the fifth-order outer terms $\widetilde{\boldsymbol{E}}_5$ and $\widetilde{\boldsymbol{H}}_5$ are given by

$$\begin{aligned}
\widetilde{\boldsymbol{E}}_5(x) = \frac{3\kappa^5}{10} h_1^{(1)}(\kappa r)\gamma_\times[\boldsymbol{H}^{\mathrm{i}}(0)] - \frac{3\kappa^5}{10}\widetilde{h}_1^{(1)}(\kappa r)\gamma_{\mathrm{t}}[\boldsymbol{E}^{\mathrm{i}}(0)] - \frac{3\kappa^5}{5}\frac{h_1^{(1)}(\kappa r)}{i\kappa r}\gamma_{\mathrm{n}}[\boldsymbol{E}^{\mathrm{i}}(0)]\,\widehat{x} \\
- \frac{\kappa^4}{9} h_2^{(1)}(\kappa r)\gamma_\times\Big[\mathbb{J}^{\mathrm{s}}_{\boldsymbol{H}^{\mathrm{i}}}(0)\widehat{x}\Big] - \frac{\kappa^4}{6}\widetilde{h}_2^{(1)}(\kappa r)\gamma_{\mathrm{t}}\Big[\mathbb{J}^{\mathrm{s}}_{\boldsymbol{E}^{\mathrm{i}}}(0)\widehat{x}\Big] - \frac{\kappa^4}{2}\frac{h_2^{(1)}(\kappa r)}{i\kappa r}\gamma_{\mathrm{n}}\Big[\mathbb{J}_{\boldsymbol{E}^{\mathrm{i}}}(0)\widehat{x}\Big]\,\widehat{x}
\end{aligned} \tag{2.4}$$

and

$$\widetilde{\boldsymbol{H}}_5(x) = -\frac{3\kappa^5}{10} h_1^{(1)}(\kappa r)\gamma_\times[\boldsymbol{E}^{\mathrm{i}}(0)] - \frac{3\kappa^5}{10}\widetilde{h}_1^{(1)}(\kappa r)\gamma_{\mathrm{t}}[\boldsymbol{H}^{\mathrm{i}}(0)] - \frac{3\kappa^5}{5}\frac{h_1^{(1)}(\kappa r)}{i\kappa r}\gamma_{\mathrm{n}}[\boldsymbol{H}^{\mathrm{i}}(0)]\,\widehat{x}$$
$$- \frac{\kappa^4}{6} h_2^{(1)}(\kappa r)\gamma_\times\Big[\mathbb{J}^{\mathrm{s}}_{\boldsymbol{E}^{\mathrm{i}}}(0)\widehat{x}\Big] + \frac{\kappa^4}{9}\widetilde{h}_2^{(1)}(\kappa r)\gamma_{\mathrm{t}}\Big[\mathbb{J}^{\mathrm{s}}_{\boldsymbol{H}^{\mathrm{i}}}(0)\widehat{x}\Big] + \frac{\kappa^4}{3}\frac{h_2^{(1)}(\kappa r)}{i\kappa r}\gamma_{\mathrm{n}}\Big[\mathbb{J}_{\boldsymbol{H}^{\mathrm{i}}}(0)\widehat{x}\Big]\,\widehat{x}, \tag{2.5}$$

where $\mathbb{J}_{\boldsymbol{\psi}}$ denotes the Jacobian matrix of $\boldsymbol{\psi}$ for $\boldsymbol{\psi} = \boldsymbol{E}^{\mathrm{i}}$ or $\boldsymbol{H}^{\mathrm{i}}$ and $\mathbb{J}^{\mathrm{s}}_{\boldsymbol{\psi}} = \frac{1}{2}(\mathbb{J}_{\boldsymbol{\psi}} + \mathbb{J}^\top_{\boldsymbol{\psi}})$ the symmetrized Jacobian of $\boldsymbol{\psi}$. Inside the boundary layer enclosing the scatterer, the exact solution $(\boldsymbol{E}_\delta, \boldsymbol{H}_\delta)$ admits the formal asymptotic expansion

$$\boldsymbol{E}_\delta(\delta\,\cdot\,) = \widehat{\boldsymbol{E}}_0 + \delta\widehat{\boldsymbol{E}}_1 + \delta^2\widehat{\boldsymbol{E}}_2 + \dots, \qquad \boldsymbol{H}_\delta(\delta\,\cdot\,) = \widehat{\boldsymbol{H}}_0 + \delta\widehat{\boldsymbol{H}}_1 + \delta^2\widehat{\boldsymbol{H}}_2 + \dots.$$

For any $\mathrm{X} \in \widehat{\Omega} := \delta^{-1}\Omega_\delta$, the zeroth-order inner terms $\widehat{\boldsymbol{E}}_0$ and $\widehat{\boldsymbol{H}}_0$ are given by

$$\widehat{\boldsymbol{E}}_0(\mathrm{X}) = \frac{1}{\mathrm{R}^3}\Big(3\gamma_{\mathrm{n}}[\boldsymbol{E}^{\mathrm{i}}(0)]\,\widehat{x} - \boldsymbol{E}^{\mathrm{i}}(0)\Big), \qquad \widehat{\boldsymbol{H}}_0(\mathrm{X}) = -\frac{1}{2\mathrm{R}^3}\Big(3\gamma_{\mathrm{n}}[\boldsymbol{H}^{\mathrm{i}}(0)]\,\widehat{x} - \boldsymbol{H}^{\mathrm{i}}(0)\Big), \tag{2.6}$$

with $\mathrm{X} = \mathrm{R}\widehat{x}$ and $\mathrm{R} = \delta^{-1}r$. Moreover, for any $\mathrm{X} \in \widehat{\Omega}$, the first-order inner terms $\widehat{\boldsymbol{E}}_1$ and $\widehat{\boldsymbol{H}}_1$ are given by

$$\begin{aligned}\widehat{\boldsymbol{E}}_1(\mathrm{X}) &= \frac{1}{\mathrm{R}^4}\Big(-\gamma_{\mathrm{t}}[\mathbb{J}^{\mathrm{s}}_{\boldsymbol{E}^{\mathrm{i}}}(0)\,\widehat{x}] + \frac{3}{2}\gamma_{\mathrm{n}}[\mathbb{J}_{\boldsymbol{E}^{\mathrm{i}}}(0)\,\widehat{x}]\,\widehat{x}\Big) + \frac{i\kappa}{2\mathrm{R}^2}\,\gamma_\times[\boldsymbol{H}^{\mathrm{i}}(0)],\\ \widehat{\boldsymbol{H}}_1(\mathrm{X}) &= \frac{1}{\mathrm{R}^4}\Big(\frac{2}{3}\gamma_{\mathrm{t}}[\mathbb{J}^{\mathrm{s}}_{\boldsymbol{H}^{\mathrm{i}}}(0)\,\widehat{x}] - \gamma_{\mathrm{n}}[\mathbb{J}_{\boldsymbol{H}^{\mathrm{i}}}(0)\,\widehat{x}]\,\widehat{x}\Big) + \frac{i\kappa}{\mathrm{R}^2}\,\gamma_\times[\boldsymbol{E}^{\mathrm{i}}(0)].\end{aligned} \tag{2.7}$$

Finally, for any $\mathrm{X} \in \widehat{\Omega}$, the second-order inner terms $\widehat{\boldsymbol{E}}_2$ and $\widehat{\boldsymbol{H}}_2$ are given by

$$\begin{aligned}\widehat{\boldsymbol{E}}_2(\mathrm{X}) = \frac{1}{\mathrm{R}^5}\Big(&\frac{2}{3}\gamma_{\mathrm{n}}[\widehat{x}^\top\mathbb{H}_{\boldsymbol{E}^{\mathrm{i}}}(0)\,\widehat{x}]\,\widehat{x} + \frac{2\kappa^2}{15}\gamma_{\mathrm{n}}[\boldsymbol{E}^{\mathrm{i}}(0)]\,\widehat{x} - \frac{1}{2}\gamma_{\mathrm{t}}[\widehat{x}^\top\mathbb{H}_{\boldsymbol{E}^{\mathrm{i}}}(0)\,\widehat{x}]\\ &- \frac{i\kappa}{3}\gamma_\times[\mathbb{J}^{\mathrm{s}}_{\boldsymbol{H}^{\mathrm{i}}}(0)\,\widehat{x}] - \frac{\kappa^2}{5}\gamma_{\mathrm{t}}[\boldsymbol{E}^{\mathrm{i}}(0)]\Big) + \frac{i\kappa}{3\mathrm{R}^3}\gamma_\times[\mathbb{J}^{\mathrm{s}}_{\boldsymbol{H}^{\mathrm{i}}}(0)\,\widehat{x}]\\ &- \frac{3\kappa^2}{10\mathrm{R}^3}\Big(\boldsymbol{E}^{\mathrm{i}}(0) - 3\gamma_{\mathrm{n}}[\boldsymbol{E}^{\mathrm{i}}(0)]\,\widehat{x}\Big) + \frac{\kappa^2}{2\mathrm{R}}\Big(\boldsymbol{E}^{\mathrm{i}}(0) + \gamma_{\mathrm{n}}[\boldsymbol{E}^{\mathrm{i}}(0)]\,\widehat{x}\Big)\end{aligned}$$

and

$$\begin{aligned}\widehat{\boldsymbol{H}}_2(\mathrm{X}) = \frac{1}{\mathrm{R}^5}\Big(&-\frac{1}{2}\gamma_{\mathrm{n}}[\widehat{x}^\top\,\mathbb{H}_{\boldsymbol{H}^{\mathrm{i}}}(0)\,\widehat{x}]\,\widehat{x} - \frac{\kappa^2}{10}\gamma_{\mathrm{n}}[\boldsymbol{H}^{\mathrm{i}}(0)]\,\widehat{x} + \frac{3}{8}\gamma_{\mathrm{t}}[\widehat{x}^\top\mathbb{H}_{\boldsymbol{H}^{\mathrm{i}}}(0)\widehat{x}]\\ &- \frac{i\kappa}{4}\gamma_\times[\mathbb{J}^{\mathrm{s}}_{\boldsymbol{E}^{\mathrm{i}}}(0)\widehat{x}] + \frac{3\kappa^2}{20}\gamma_{\mathrm{t}}[\boldsymbol{H}^{\mathrm{i}}(0)]\Big) + \frac{i\kappa}{2\mathrm{R}^3}\gamma_\times[\mathbb{J}^{\mathrm{s}}_{\boldsymbol{E}^{\mathrm{i}}}(0)\,\widehat{x}]\\ &+ \frac{3\kappa^2}{10\mathrm{R}^3}\Big(3\gamma_{\mathrm{n}}[\boldsymbol{H}^{\mathrm{i}}(0)]\,\widehat{x} - \boldsymbol{H}^{\mathrm{i}}(0)\Big) - \frac{\kappa^2}{4\mathrm{R}}\Big(\boldsymbol{H}^{\mathrm{i}}(0) + \gamma_{\mathrm{n}}[\boldsymbol{H}^{\mathrm{i}}(0)]\,\widehat{x}\Big),\end{aligned}$$

where $\mathbb{H}_\diamond$ denotes the Hessian tensor of $\diamond$, see Remark 2.

Remark 2. For any $x = (x_1, x_2, x_3)^\top \in \mathbb{R}^3$ and $\boldsymbol{f} = (f_1, f_2, f_3)^\top$, the vector field $x^\top\mathbb{H}_f(0)x$ is defined by its componentwise

$$\Big(x^\top\mathbb{H}_f(0)x\Big)_i = \sum_{j=1}^{3}\sum_{k=1}^{3} x_k(\partial_k\partial_j f_i(0))x_j, \qquad i = 1, 2, 3.$$

Remark 3. The rigorous definition of domains of validity for the two local approximations is typically imposed by the method of matched asymptotic expansions and is introduced in numerous publications [14, 15, 20, 21, 23, 33]. In practice, we can take the two overlapping domains $\left\{x \in \mathbb{R}^3,\ |x| > \sqrt{\delta\lambda}\right\}$ and $\left\{\mathrm{X} \in \mathbb{R}^3,\ \delta < \delta|\mathrm{X}| < 2\sqrt{\delta\lambda}\right\}$ respectively for the validity of the outer and inner approximation.

3. Physical interpretation: Identification of equivalent multipoles

Successive terms of the asymptotic expansions can be interpreted as electromagnetic fields generated by electromagnetic multipoles. The multipolar sources are well-known in electromagnetism [38, 39] and are characterized by moments [33, Appendix B]. Time-harmonic multipoles come from time-dependent multipoles and the computation of electromagnetic fields is based on the theory of retarded potentials, by taking into account the phase differences.

3.1. Time-harmonic and static dipoles

3.1.1. Time-harmonic electric dipole

The time-harmonic electromagnetic fields $\boldsymbol{\mathcal{E}}_{\mathrm{e}}[\mathbf{d}]$ and $\boldsymbol{\mathcal{H}}_{\mathrm{e}}[\mathbf{d}]$ generated by an electric dipole of moment $\mathbf{d} \in \mathbb{C}^3$ are given by

$$\begin{aligned} \boldsymbol{\mathcal{E}}_{\mathrm{e}}[\mathbf{d}](x) &= \frac{\exp(i\kappa r)}{4\pi r}\left\{2\left(\frac{1}{r^2}-\frac{i\kappa}{r}\right)\gamma_{\mathrm{n}}[\mathbf{d}]\,\widehat{x} - \left(\frac{1}{r^2}-\frac{i\kappa}{r}-\kappa^2\right)\gamma_{\mathrm{t}}[\mathbf{d}]\right\}, \\ \boldsymbol{\mathcal{H}}_{\mathrm{e}}[\mathbf{d}](x) &= \frac{\exp(i\kappa r)}{4\pi r}\left(\kappa^2+\frac{i\kappa}{r}\right)\gamma_{\times}[\mathbf{d}]. \end{aligned} \tag{3.1}$$

Remark 4. We recognize in (3.1) the Hankel functions of the first kind of order 1, so we can rewrite (3.1) as

$$\boldsymbol{\mathcal{E}}_{\mathrm{e}}[\mathbf{d}](x) = -\frac{\kappa^3}{4\pi}\left(\widetilde{h}_1^{(1)}(\kappa r)\,\gamma_{\mathrm{t}}[\mathbf{d}] + 2\frac{h_1^{(1)}(\kappa r)}{i\kappa r}\gamma_{\mathrm{n}}[\mathbf{d}]\,\widehat{x}\right), \qquad \boldsymbol{\mathcal{H}}_{\mathrm{e}}[\mathbf{d}](x) = -\frac{\kappa^3}{4\pi}h_1^{(1)}(\kappa r)\gamma_{\times}[\mathbf{d}].$$

The dipolar moment $\mathbf{d}$ can be a complex vector. In that case, the dipole moment can be seen like a superposition of three out of time-phase dipole moments,

$$\mathbf{d} = \sum_{k=1}^{3} d_k\ \exp(-i\omega\tau_k)\,\boldsymbol{e}_k,$$

where $(\boldsymbol{e}_1, \boldsymbol{e}_2, \boldsymbol{e}_3)$ denotes the canonical basis of $\mathbb{R}^3$, $d_k = |\mathbf{d}\cdot\boldsymbol{e}_k|$ denotes the k-th dipole amplitude and $\tau_k = -\omega^{-1}\arg(\mathbf{d}\cdot\boldsymbol{e}_k)$ the k-th time-related phase difference, where $\arg(\mathbf{d}\cdot\boldsymbol{e}_k)$ is chosen into $(0, 2\pi)$. It is worth noting that the choice of basis is arbitrary. A dipole of moment $\mathbf{d} \in \mathbb{R}^3$ can be defined by an asymptotic process including a geometrical point of view: let ϵ be a real positive number and consider the electromagnetic fields $\boldsymbol{\mathcal{E}}_{\epsilon}[\mathbf{d}]$ and $\boldsymbol{\mathcal{H}}_{\epsilon}[\mathbf{d}]$ generated by a distribution of two electric point-charges, located at $+\frac{\epsilon}{2}\mathbf{d}$ and $-\frac{\epsilon}{2}\mathbf{d}$, and an electric filiform current relating the two point-charges, see Figure 2. The electromagnetic fields $\boldsymbol{\mathcal{E}}_{\epsilon}[\mathbf{d}]$ and $\boldsymbol{\mathcal{H}}_{\epsilon}[\mathbf{d}]$ have the following asymptotic behavior

$$\boldsymbol{\mathcal{E}}_{\epsilon}[\mathbf{d}] = \boldsymbol{\mathcal{E}}_{\mathrm{e}}[\mathbf{d}] + \underset{\epsilon\to0}{O}(\epsilon), \qquad \boldsymbol{\mathcal{H}}_{\epsilon}[\mathbf{d}] = \boldsymbol{\mathcal{H}}_{\mathrm{e}}[\mathbf{d}] + \underset{\epsilon\to0}{O}(\epsilon),$$

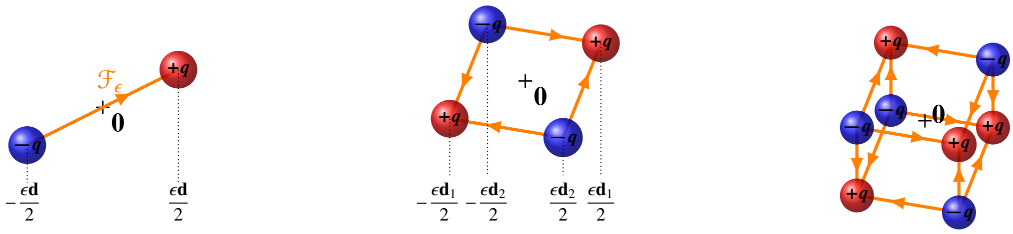

Figure 2: Dipolar, quadrupolar and octupolar configurations

and solve the following time-harmonic Maxwell problem in the sense of distributions,

$$\begin{cases} \nabla\times\boldsymbol{\mathcal{E}}_\epsilon[\mathbf{d}] - i\kappa\boldsymbol{\mathcal{H}}_\epsilon[\mathbf{d}] = 0 & \text{in } \mathscr{D}'(\mathbb{R}^3), \\ \nabla\times\boldsymbol{\mathcal{H}}_\epsilon[\mathbf{d}] + i\kappa\boldsymbol{\mathcal{E}}_\epsilon[\mathbf{d}] = \dfrac{1}{c}\,\mathbf{j}_\epsilon[\mathbf{d}] & \text{in } \mathscr{D}'(\mathbb{R}^3), \\ \nabla\cdot\boldsymbol{\mathcal{E}}_\epsilon[\mathbf{d}] = \varrho_\epsilon[\mathbf{d}] & \text{in } \mathscr{D}'(\mathbb{R}^3), \\ \nabla\cdot\boldsymbol{\mathcal{H}}_\epsilon[\mathbf{d}] = 0 & \text{in } \mathscr{D}'(\mathbb{R}^3), \end{cases} \tag{3.2}$$

where the charge density $\varrho_\epsilon[\mathbf{d}]$ and the current density $\mathbf{j}_\epsilon[\mathbf{d}]$ which satisfy the charge conservation principle are the distributions given by

$$\varrho_\epsilon[\mathbf{d}] = \frac{q}{\epsilon}\left(\delta_{+\frac{\epsilon}{2}\mathbf{d}} - \delta_{-\frac{\epsilon}{2}\mathbf{d}}\right), \qquad \mathbf{j}_\epsilon[\mathbf{d}] = \frac{i\omega q}{\epsilon}\frac{\mathbf{d}}{|\mathbf{d}|}\,\delta_{\mathcal{F}_\epsilon}.$$

The electric dipole problem is the limit when ϵ tends to zero of (3.2),

$$\begin{cases} \nabla\times\boldsymbol{\mathcal{E}}[\mathbf{d}] - i\kappa\boldsymbol{\mathcal{H}}[\mathbf{d}] = 0 & \text{in } \mathscr{D}'(\mathbb{R}^3), \\ \nabla\times\boldsymbol{\mathcal{H}}[\mathbf{d}] + i\kappa\boldsymbol{\mathcal{E}}[\mathbf{d}] = i\kappa\,\mathbf{d}\,\delta_0 & \text{in } \mathscr{D}'(\mathbb{R}^3), \\ \nabla\cdot\boldsymbol{\mathcal{E}}[\mathbf{d}] = D\delta_0[\mathbf{d}] & \text{in } \mathscr{D}'(\mathbb{R}^3), \\ \nabla\cdot\boldsymbol{\mathcal{H}}[\mathbf{d}] = 0 & \text{in } \mathscr{D}'(\mathbb{R}^3). \end{cases} \tag{3.3}$$

where $\delta_\diamond$ denotes the Dirac distribution at point $\diamond\in\mathbb{R}^3$ and $D\delta_0[\mathbf{d}]$ stands for the differential of δ_0 in the direction $\mathbf{d}$, defined in the sense of distributions by

$$\langle D\delta_0[\mathbf{d}], f\rangle = -\langle\delta_0, \nabla f\cdot\mathbf{d}\rangle = -\nabla f(0)\cdot\mathbf{d} \qquad \forall f\in\mathscr{D}(\mathbb{R}^3).$$

The case where the Dirac distribution is evaluated on the one-dimensional wire $\mathcal{F}_\epsilon$ is defined by

$$\langle\delta_{\mathcal{F}_\epsilon}, f\rangle = \int_{\mathcal{F}_\epsilon} f(x)\,dx \qquad \forall f\in\mathscr{D}(\mathbb{R}^3).$$

3.1.2. Time-harmonic magnetic dipole

The time-harmonic electromagnetic fields $\boldsymbol{\mathcal{E}}_{\mathrm{m}}[\mathbf{d}]$ and $\boldsymbol{\mathcal{H}}_{\mathrm{m}}[\mathbf{d}]$ generated by a magnetic dipole of moment $\mathbf{d}\in\mathbb{C}^3$ are given by

$$\boldsymbol{\mathcal{E}}_{\mathrm{m}}[\mathbf{d}](x) = \frac{\kappa^3}{4\pi}h_1^{(1)}(\kappa r)\gamma_\times[\mathbf{d}], \quad \boldsymbol{\mathcal{H}}_{\mathrm{m}}[\mathbf{d}](x) = -\frac{\kappa^3}{4\pi}\left(\widetilde{h}_1^{(1)}(\kappa r)\,\gamma_{\mathrm{t}}[\mathbf{d}] + 2\frac{h_1^{(1)}(\kappa r)}{i\kappa r}\gamma_{\mathrm{n}}[\mathbf{d}]\,\widehat{x}\right). \tag{3.4}$$

A magnetic dipole is defined analogously to an electric dipole by replacing the electric sources of (3.3), by magnetic sources into the Maxwell-Faraday equation (the first one of (3.3)) and the Maxwell-Thomson equation (the last one of (3.3)).

3.1.3. Quasi-static dipoles

Electrostatic field generated by an electric dipole. The electric field $\boldsymbol{\mathcal{E}}_{0,\mathrm{e}}[\mathbf{d}]$ generated by an electrostatic dipole of moment $\mathbf{d} \in \mathbb{C}^3$ is given by

$$\boldsymbol{\mathcal{E}}_{0,\mathrm{e}}[\mathbf{d}](x) = \frac{1}{4\pi r^3}\left(2\gamma_{\mathrm{n}}[\mathbf{d}]\,\widehat{x} - \gamma_{\mathrm{t}}[\mathbf{d}]\right). \tag{3.5}$$

This expression matches with (3.1) for $\omega = 0$. Indeed, the electrostatic dipole correcponds to the electric dipole (3.3) with $\omega = 0$,

$$\begin{cases} \nabla \cdot \boldsymbol{\mathcal{E}}[\mathbf{d}] = D\delta_0[\mathbf{d}] & \text{in } \mathscr{D}'(\mathbb{R}^3), \\ \nabla \times \boldsymbol{\mathcal{E}}[\mathbf{d}] = 0 & \text{in } \boldsymbol{\mathscr{D}}'(\mathbb{R}^3). \end{cases}$$

Quasi-static magnetic field generated by an electric dipole. The magnetic field $\boldsymbol{\mathcal{H}}_{0,\mathrm{e}}[\mathbf{d}]$ generated by a quasi-static electric dipole of moment $\mathbf{d} = \frac{1}{i\kappa}\mathbf{d}_\kappa \in \mathbb{C}^3$ is given by

$$\boldsymbol{\mathcal{H}}_{0,\mathrm{e}}[\mathbf{d}](x) = -\frac{1}{4\pi r^2}\gamma_\times[\mathbf{d}_\kappa].$$

The problem satisfied by the quasi-static magnetic field $\boldsymbol{\mathcal{H}}_{0,\mathrm{e}}[\mathbf{d}]$ is obtained by taking $\omega = 0$ into the magnetic equations of the electric dipole problem (3.3),

$$\begin{cases} \nabla \cdot \boldsymbol{\mathcal{H}}[\mathbf{d}] = 0 & \text{in } \mathscr{D}'(\mathbb{R}^3), \\ \nabla \times \boldsymbol{\mathcal{H}}[\mathbf{d}] = \mathbf{d}_\kappa\,\boldsymbol{\delta}_0 & \text{in } \boldsymbol{\mathscr{D}}'(\mathbb{R}^3). \end{cases}$$

Extension to magnetic dipoles. The quasi-static electric field $\boldsymbol{\mathcal{E}}_{0,\mathrm{m}}[\mathbf{d}]$ and the magnetostatic field $\boldsymbol{\mathcal{H}}_{0,\mathrm{m}}[\mathbf{d}]$ generated by a magnetic dipole of moment $\mathbf{d} = \frac{1}{i\kappa}\mathbf{d}_\kappa \in \mathbb{C}^3$ read as

$$\boldsymbol{\mathcal{H}}_{0,\mathrm{m}}[\mathbf{d}](x) = \frac{1}{4\pi r^3}\left(2\gamma_{\mathrm{n}}[\mathbf{d}]\,\widehat{x} - \gamma_{\mathrm{t}}[\mathbf{d}]\right), \qquad \boldsymbol{\mathcal{E}}_{0,\mathrm{m}}[\mathbf{d}](x) = \frac{1}{4\pi r^2}\gamma_\times[\mathbf{d}_\kappa].$$

3.2. Time-harmonic and static quadrupoles

3.2.1. Time-harmonic electric quadrupole

The time-harmonic electromagnetic fields $\boldsymbol{\mathcal{E}}_{\mathrm{e}}[\mathbf{Q}]$ and $\boldsymbol{\mathcal{H}}_{\mathrm{e}}[\mathbf{Q}]$ generated by an electric quadrupole of moment tensor $\mathbf{Q}$ are given by

$$\boldsymbol{\mathcal{E}}_{\mathrm{e}}[\mathbf{Q}](x) = \frac{\kappa^4}{16\pi}\left(\frac{3\,h_2^{(1)}(\kappa r)}{i\kappa r}\gamma_{\mathrm{n}}[\mathbf{Q}\widehat{x}]\,\widehat{x} + \widetilde{h}_2^{(1)}(\kappa r)\gamma_{\mathrm{t}}[\mathbf{Q}\widehat{x}]\right), \quad \boldsymbol{\mathcal{H}}_{\mathrm{e}}[\mathbf{Q}](x) = -\frac{\kappa^4}{16\pi}h_2^{(1)}(\kappa r)\gamma_\times[\mathbf{Q}\widehat{x}]. \tag{3.6}$$

The quadrupole moment tensor $\mathbf{Q}$ is a traceless and symmetric complex-valued two-rank tensor [38]. Generally, a quadrupole can be decomposed as the superposition of five out of time-phase quadrupoles,

$$\mathbf{Q} = \sum_{k=1}^{5} m_k\,\exp(-i\omega\tau_k)\,\mathbf{M}_k,$$

where m_k denotes the elementary amplitude, τ_k is the time-related phase difference and $(\mathbf{M}_k)_{k=1,\ldots,5}$ is an arbitrary basis of elementary quadrupole tensors. A suitable basis is given by

$$\mathbf{M}_1 = \begin{pmatrix} 1 & 0 & 0 \\ 0 & 0 & 0 \\ 0 & 0 & -1 \end{pmatrix}, \ \mathbf{M}_2 = \begin{pmatrix} 0 & 0 & 0 \\ 0 & 1 & 0 \\ 0 & 0 & -1 \end{pmatrix}, \ \mathbf{M}_3 = \begin{pmatrix} 0 & 1 & 0 \\ 1 & 0 & 0 \\ 0 & 0 & 0 \end{pmatrix}, \ \mathbf{M}_4 = \begin{pmatrix} 0 & 0 & 1 \\ 0 & 0 & 0 \\ 1 & 0 & 0 \end{pmatrix}, \ \mathbf{M}_5 = \begin{pmatrix} 0 & 0 & 0 \\ 0 & 0 & 1 \\ 0 & 1 & 0 \end{pmatrix}.$$

Each elementary tensor $\mathbf{M}_k$ can be expressed as

$$\mathbf{M}_k = \frac{1}{2}\left(\mathbf{u}_k\mathbf{v}_k^\top + \mathbf{v}_k\mathbf{u}_k^\top\right)$$

where $\mathbf{u}_k, \mathbf{v}_k \in \mathbb{R}^3$, illustrated in Figure 3, are given by $\mathbf{u}_1 = (1,0,1)^\top$, $\mathbf{v}_1 = (1,0,-1)^\top$, $\mathbf{u}_2 = (0,1,1)^\top$, $\mathbf{v}_2 = (0,1,-1)^\top$, $\mathbf{u}_3 = (1,0,0)^\top$, $\mathbf{v}_3 = \mathbf{u}_2 + \mathbf{v}_2$, $\mathbf{u}_4 = \mathbf{u}_3$, $\mathbf{v}_4 = (0,0,2)^\top$, $\mathbf{u}_5 = (0,1,0)^\top$, $\mathbf{v}_5 = \mathbf{v}_4$.

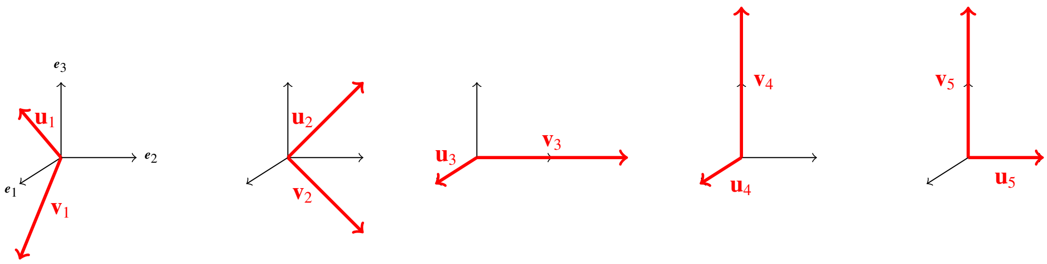

Figure 3: A basis of real-valued quadrupoles defined by the elementary directions $\mathbf{u}_k$ and $\mathbf{v}_k$ associated with the basis of elementary quadrupole moment tensors $\mathbf{M}_k$.

Remark 5. It is also possible to normalize both $\mathbf{u}_k$ and $\mathbf{v}_k$ but it leads to a different quadrupole moment tensor basis $\widetilde{\mathbf{M}}_k = \frac{1}{2}\mathbf{M}_k$.

Each quadrupole of real-valued moment tensor $\mathbf{M}_k$ can be interpreted thanks to an asymptotic process with a geometrical point of view. Let $\epsilon > 0$ and consider the electromagnetic fields $\boldsymbol{\mathcal{E}}_\epsilon[\mathbf{u}_k, \mathbf{v}_k]$ and $\boldsymbol{\mathcal{H}}_\epsilon[\mathbf{u}_k, \mathbf{v}_k]$ generated by a distribution of four electric point-charges, two positive ones located at $\pm\frac{\epsilon}{2}\mathbf{d}_1^k$ where $\mathbf{d}_1^k = \frac{1}{2}(\mathbf{v}_k - \mathbf{u}_k)$, two negative ones located at $\pm\frac{\epsilon}{2}\mathbf{d}_2^k$ where $\mathbf{d}_2^k = \frac{1}{2}(\mathbf{u}_k + \mathbf{v}_k)$, and four electric filiform currents connecting the four point-charges, see Figure 2. As a result, the electromagnetic fields have the following asymptotic behavior,

$$\boldsymbol{\mathcal{E}}_\epsilon[\mathbf{u}_k, \mathbf{v}_k] = \boldsymbol{\mathcal{E}}_{\mathrm{e}}[\mathbf{Q}_k] + \underset{\epsilon\to 0}{O}(\epsilon), \qquad \boldsymbol{\mathcal{H}}_\epsilon[\mathbf{u}_k, \mathbf{v}_k] = \boldsymbol{\mathcal{H}}_{\mathrm{e}}[\mathbf{Q}_k] + \underset{\epsilon\to 0}{O}(\epsilon)$$

and solve the following time-harmonic Maxwell problem,

$$\begin{cases} \nabla \times \boldsymbol{\mathcal{E}}_\epsilon[\mathbf{u}_k, \mathbf{v}_k] - i\kappa\boldsymbol{\mathcal{H}}_\epsilon[\mathbf{u}_k, \mathbf{v}_k] = 0 & \text{in } \mathscr{D}'(\mathbb{R}^3), \\ \nabla \times \boldsymbol{\mathcal{H}}_\epsilon[\mathbf{u}_k, \mathbf{v}_k] + i\kappa\boldsymbol{\mathcal{E}}_\epsilon[\mathbf{u}_k, \mathbf{v}_k] = \dfrac{1}{c}\,\mathbf{j}_\epsilon[\mathbf{d}_1^k, \mathbf{d}_2^k] & \text{in } \mathscr{D}'(\mathbb{R}^3), \\ \nabla \cdot \boldsymbol{\mathcal{E}}_\epsilon[\mathbf{u}_k, \mathbf{v}_k] = \varrho_\epsilon[\mathbf{d}_1^k, \mathbf{d}_2^k] & \text{in } \mathscr{D}'(\mathbb{R}^3), \\ \nabla \cdot \boldsymbol{\mathcal{H}}_\epsilon[\mathbf{u}_k, \mathbf{v}_k] = 0 & \text{in } \mathscr{D}'(\mathbb{R}^3), \end{cases}$$

where the charge density $\varrho_\epsilon[\mathbf{d}_1^k, \mathbf{d}_2^k]$ is the distribution given by

$$\varrho_\epsilon[\mathbf{d}_1^k, \mathbf{d}_2^k] = \frac{q}{\epsilon^2}\left(\boldsymbol{\delta}_{+\frac{\epsilon}{2}\mathbf{d}_1^k} + \boldsymbol{\delta}_{-\frac{\epsilon}{2}\mathbf{d}_1^k} - \boldsymbol{\delta}_{+\frac{\epsilon}{2}\mathbf{d}_2^k} - \boldsymbol{\delta}_{-\frac{\epsilon}{2}\mathbf{d}_2^k}\right) \tag{3.7}$$

and $\mathbf{j}_\epsilon[\mathbf{d}_1^k, \mathbf{d}_2^k]$ is defined to satisfy the charge conservation principle.

3.2.2. Time-harmonic magnetic quadrupole

The time-harmonic electromagnetic fields $\boldsymbol{\mathcal{E}}_{\mathrm{m}}[\mathbf{Q}]$ and $\boldsymbol{\mathcal{H}}_{\mathrm{m}}[\mathbf{Q}]$ generated by a magnetic quadrupole of moment tensor $\mathbf{Q}$ are given by

$$\begin{aligned}
\boldsymbol{\mathcal{H}}_{\mathrm{m}}[\mathbf{Q}](x) &= \frac{\kappa^4}{16\pi}\left(\frac{3\,h_2^{(1)}(\kappa r)}{i\kappa r}\gamma_{\mathrm{n}}[\mathbf{Q}\widehat{x}]\widehat{x} + \widetilde{h}_2^{(1)}(\kappa r)\gamma_{\mathrm{t}}[\mathbf{Q}\widehat{x}]\right),\\
\boldsymbol{\mathcal{E}}_{\mathrm{m}}[\mathbf{Q}](x) &= \frac{\kappa^4}{16\pi}h_2^{(1)}(\kappa r)\gamma_\times[\mathbf{Q}\widehat{x}].
\end{aligned}$$

3.2.3. Electrostatic quadrupole

The electric field $\boldsymbol{\mathcal{E}}_{0,\mathrm{e}}[\mathbf{Q}]$ generated by an electrostatic quadrupole is given by

$$\boldsymbol{\mathcal{E}}_{0,\mathrm{e}}[\mathbf{Q}](x) = \frac{3}{16\pi r^4}\left(-3\gamma_{\mathrm{n}}[\mathbf{Q}\widehat{x}]\,\widehat{x} + \gamma_{\mathrm{t}}[\mathbf{Q}\widehat{x}]\right).$$

This expression matches with (3.6) for $\omega = 0$. The electrostatic quadrupole is defined analogously to electrostatic dipole by considering the charge density (3.7),

$$\begin{cases}
\nabla\cdot\boldsymbol{\mathcal{E}}[\mathbf{u},\mathbf{v}] = D^2\boldsymbol{\delta}_0[\mathbf{d}_1,\mathbf{d}_2] & \text{in } \mathscr{D}'(\mathbb{R}^3),\\
\nabla\times\boldsymbol{\mathcal{E}}[\mathbf{u},\mathbf{v}] = 0 & \text{in } \mathscr{D}'(\mathbb{R}^3),
\end{cases}$$

where the distribution $D^2\boldsymbol{\delta}_0[\mathbf{d}_1,\mathbf{d}_2]$ denotes the second-order derivative of $\boldsymbol{\delta}_0$ in the directions $\mathbf{d}_1$ and $\mathbf{d}_2$ defined in the sense of distributions.

3.3. Interpretation of the asymptotic expansions in terms of multipoles

Proposition 1. *The electric inner term $\widehat{\boldsymbol{E}}_0$ given by* (2.6) *can be identified with* (3.5)*, a static electric field generated by an electric dipole of moment $\mathbf{d}_{\mathrm{E}} = 4\pi\boldsymbol{E}^i(0)$. The magnetic inner term $\widehat{\boldsymbol{H}}_0$ given by* (2.6) *can be identified with a static magnetic field generated by a magnetic dipole of moment $\mathbf{d}_{\mathrm{H}} = -2\pi\boldsymbol{H}^i(0)$.*

Proposition 2. *The inner terms $\widehat{\boldsymbol{E}}_1$ and $\widehat{\boldsymbol{H}}_1$ in* (2.7) *can be identified with the superposition of*

- *a static electric (resp. magnetic) field generated by a magnetic (resp. electric) filiform current connecting two point-charges of moment $\mathbf{d}_{\mathrm{H}}$ (resp. $\mathbf{d}_{\mathrm{E}}$), given by Proposition 1,*
- *a static electric (resp. magnetic) field generated by an electric (resp. magnetic) quadrupole of moment tensor $\mathbf{Q}_{\mathrm{E}} = -\frac{8\pi}{3}\mathbb{J}^s_{\boldsymbol{E}^i}(0)$ (resp. $\mathbf{Q}_{\mathrm{H}} = \frac{16\pi}{9}\mathbb{J}^s_{\boldsymbol{H}^i}(0)$), where $\mathbb{J}^s_\diamond = \frac{1}{2}(\mathbb{J}_\diamond + \mathbb{J}_\diamond^\top)$ denotes the symmetric part of the Jacobian matrix of $\diamond$.*

Remark 6. The second-order inner terms $\widehat{\boldsymbol{E}}_2$ and $\widehat{\boldsymbol{H}}_2$ are a superposition of octupoles, quadrupoles and dipoles.

Proposition 3. *The outer terms* $\widetilde{\boldsymbol{E}}_3$ *and* $\widetilde{\boldsymbol{H}}_3$ *given by* (2.3) *can be identified with the superposition of an electric (resp. magnetic) field generated by an electric dipole of moment* $\mathbf{d}_{\mathrm{E}}$ *and an electric (resp. magnetic) field generated by a magnetic dipole of moment* $\mathbf{d}_{\mathrm{H}}$*.*

Proposition 4. *The outer terms* $\widetilde{\boldsymbol{E}}_5$ *and* $\widetilde{\boldsymbol{H}}_5$ *given by* (2.4) *and* (2.5) *can be identified with the superposition of electric fields, respectively magnetic fields, generated by an electric dipole of moment* $\frac{3\kappa^2}{10}\mathbf{d}_{\mathrm{E}}$*, a magnetic dipole of moment* $\frac{3\kappa^2}{5}\mathbf{d}_{\mathrm{H}}$*, an electric quadrupole of moment tensor* $\mathbf{Q}_{\mathrm{E}}$ *and a magnetic quadrupole of moment tensor* $\mathbf{Q}_{\mathrm{H}}$*.*

4. Approximate models

In this section, we introduce a semi-analytical method reproducing the main properties of the asymptotic expansions:

- an accurate formula for the equivalent dipolar approximation,
- a Born approximation of the solution.

4.1. Accurate equivalent dipolar approximation: the collected model

The asymptotic expansion truncated at order P reading as

$$\delta^3\widetilde{\boldsymbol{E}}_3 + \ldots + \delta^P\widetilde{\boldsymbol{E}}_P, \qquad \delta^3\widetilde{\boldsymbol{H}}_3 + \ldots + \delta^P\widetilde{\boldsymbol{H}}_P,$$

provides an approximate solution. However, except for $\widetilde{\boldsymbol{E}}_3$ and $\widetilde{\boldsymbol{H}}_3$, the computation of asymptotic coefficients $\widetilde{\boldsymbol{E}}_p$ and $\widetilde{\boldsymbol{H}}_p$ for $p \geq 5$ involves successive derivatives of the incident fields, which are not always numerically computable. Then, a more practical approximate model should avoid terms with incident derivatives. With this in mind, the collected approximation is defined by picking terms coming from dipolar sources into (2.3)-(2.4) and neglecting terms from high-order multipoles. From a far-field point of view, the collected dipolar expansion is

$$\boldsymbol{E}_\delta \approx \alpha_{\mathrm{H}}(\delta)\boldsymbol{\mathcal{E}}_{\mathrm{m}}[\mathbf{d}_{\mathrm{H}}] + \alpha_{\mathrm{E}}(\delta)\boldsymbol{\mathcal{E}}_{\mathrm{e}}[\mathbf{d}_{\mathrm{E}}], \qquad \boldsymbol{H}_\delta \approx \alpha_{\mathrm{H}}(\delta)\boldsymbol{\mathcal{H}}_{\mathrm{e}}[\mathbf{d}_{\mathrm{E}}] + \alpha_{\mathrm{E}}(\delta)\boldsymbol{\mathcal{H}}_{\mathrm{m}}[\mathbf{d}_{\mathrm{H}}],$$

where $\boldsymbol{\mathcal{E}}_{\mathrm{e}}[\mathbf{d}_{\mathrm{E}}]$ and $\boldsymbol{\mathcal{H}}_{\mathrm{e}}[\mathbf{d}_{\mathrm{E}}]$ are given by (3.1) and $\boldsymbol{\mathcal{E}}_{\mathrm{m}}[\mathbf{d}_{\mathrm{H}}]$ and $\boldsymbol{\mathcal{H}}_{\mathrm{m}}[\mathbf{d}_{\mathrm{H}}]$ by (3.4). The coefficients $\alpha_{\mathrm{E}}(\delta)$ and $\alpha_{\mathrm{H}}(\delta)$ are given by

$$\alpha_{\mathrm{E}}(\delta) = \delta^3\left(1 + \frac{3(\kappa\delta)^2}{10}\right) \qquad \text{and} \qquad \alpha_{\mathrm{H}}(\delta) = \delta^3\left(1 - \frac{3(\kappa\delta)^2}{5}\right). \tag{4.1}$$

Regarding numerical results on Figures 10, we observe that the collected approximations are more accurate than the *first* approximations $\delta^3\widetilde{\boldsymbol{E}}_3$ and $\delta^3\widetilde{\boldsymbol{H}}_3$. Furthermore, the collected models have a lower computational cost than the *second* approximations $\delta^3\widetilde{\boldsymbol{E}}_3 + \delta^5\widetilde{\boldsymbol{E}}_5$ and $\delta^3\widetilde{\boldsymbol{H}}_3 + \delta^5\widetilde{\boldsymbol{H}}_5$.

4.2. Born approximation

The Born approximation considers single scattering by multiple obstacles. It is based on a superposition principle of scattered fields generated in the presence of obstacles in isolated configurations [40]. The solution of multiple electromagnetic scattering problem by K non-overlapping small spheres is approximated by

$$\boldsymbol{E}_\delta \approx \sum_{k=1}^{K}\boldsymbol{E}_{\delta,k}, \qquad \boldsymbol{H}_\delta \approx \sum_{k=1}^{K}\boldsymbol{H}_{\delta,k}.$$

For $k = 1, \ldots, K$, the scattered fields $\boldsymbol{E}_{\delta,k}$ and $\boldsymbol{H}_{\delta,k}$ approximate the solution of the exterior Maxwell problem in $\mathbb{R}^3 \setminus \overline{\mathcal{B}(c_k, \delta)}$. We use the asymptotic expansions derived for the single scattering case transposed at the center c_k of each obstacle,

$$\begin{aligned}\boldsymbol{E}_{\delta,k}(x) &= \alpha_{\mathrm{H}}(\delta)\boldsymbol{\mathcal{E}}_{\mathrm{m}}[\mathbf{d}_{\mathrm{H}}^k](x - c_k) + \alpha_{\mathrm{E}}(\delta)\boldsymbol{\mathcal{E}}_{\mathrm{e}}[\mathbf{d}_{\mathrm{E}}^k](x - c_k),\\ \boldsymbol{H}_{\delta,k}(x) &= \alpha_{\mathrm{H}}(\delta)\boldsymbol{\mathcal{H}}_{\mathrm{e}}[\mathbf{d}_{\mathrm{E}}^k](x - c_k) + \alpha_{\mathrm{E}}(\delta)\boldsymbol{\mathcal{H}}_{\mathrm{m}}[\mathbf{d}_{\mathrm{H}}^k](x - c_k),\end{aligned}$$

where the coefficients $\alpha_{\mathrm{E}}(\delta)$ and $\alpha_{\mathrm{H}}(\delta)$ are given by (4.1), $\mathbf{d}_{\mathrm{E}}^k = 4\pi\boldsymbol{E}^{\mathrm{i}}(c_k)$ and $\mathbf{d}_{\mathrm{H}}^k = -2\pi\boldsymbol{H}^{\mathrm{i}}(c_k)$. Figure 4 shows a numerical simulation illustrating the Born approximation with $K = 13$ obstacles of radius $\delta = 0.1$. The incident field is an electromagnetic plane wave defined by (5.1) whose physical parameters are given by (5.2) with $\lambda = 1$. The Born approximation gives analytical

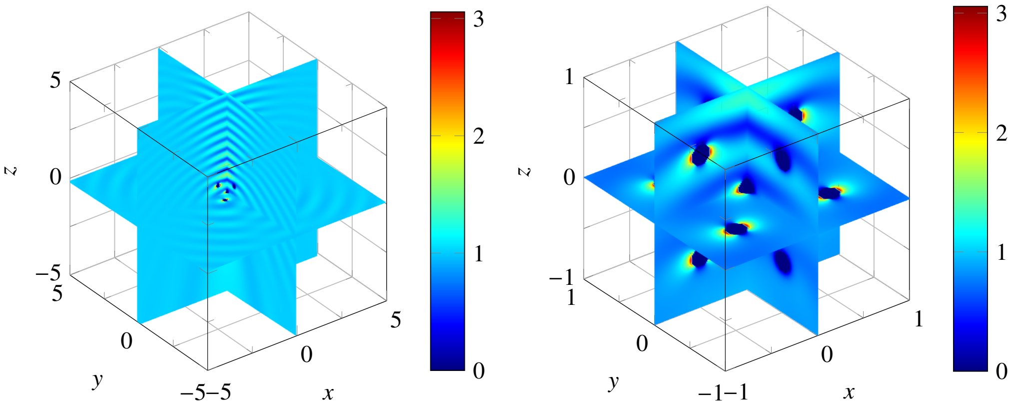

Figure 4: Cross-sections of modulus of x-component of the approximate total electric field

approximations with an explicit formulation (there is no matrix to invert). However, it appears to be unaccurate as the number of obstacles grows or the distance between the obstacles decreases.

Remark 7. This approach can be modified in the context of multiple scattering. In order to take into account the interactions between the obstacles, we need to define locally for each obstacle the local incident field acting on this obstacle. In contrast with the single scattering case where the local incident field is trivially the global incident field, the multiple scattering approach consists in considering all the other scattered fields as a new source for the local obstacle. This leads to the Foldy-Lax model [23, 25, 26], also brought in [33, Section 5.3] for electromagnetic scattering.

5. Numerical simulations

Numerical results make evident orders of convergence for different levels of inner and outer approximations. To illustrate the results, we propose two test-cases. The first one considers an incident plane wave involving an analytical solution. In the second one, we consider an incident gaussian beam that involves a numerical approximation of spectral coefficients.

5.1. The reference solution

Test 1: Incident plane wave. The spherical obstacle is enlighted by an electromagnetic plane wave $(\boldsymbol{E}^{\mathrm{i}}, \boldsymbol{H}^{\mathrm{i}})$ of wavelength λ defined by

$$\boldsymbol{E}^{\mathrm{i}}(x) = \mathbf{p}\exp(i\mathbf{k}\cdot x), \qquad \boldsymbol{H}^{\mathrm{i}}(x) = \frac{1}{\kappa}(\mathbf{k}\times\mathbf{p})\exp(i\mathbf{k}\cdot x), \tag{5.1}$$

with $\mathbf{k}\cdot\mathbf{p} = 0$. The wave vector $\mathbf{k}$ and the polarization vector $\mathbf{p}$ are chosen such that

$$\mathbf{k} = \begin{pmatrix} 0 \\ 0 \\ -\kappa \end{pmatrix}, \qquad \mathbf{p} = \begin{pmatrix} 1 \\ 0 \\ 0 \end{pmatrix}, \tag{5.2}$$

with $\kappa = \frac{2\pi}{\lambda}$.

Test 2: Incident gaussian beam. An electromagnetic gaussian beam of waist w polarized by the vector $\mathbf{p}$ given by (5.2) and directed through the z-axis, is approximated by

$$\boldsymbol{E}^{\mathrm{i}}(x) = \frac{z_0\exp(i\kappa z)}{z_0+iz}\exp\left(-\frac{1}{2}\frac{\kappa(x^2+y^2)}{z_0+iz}\right)\mathbf{p},$$

$$\boldsymbol{H}^{\mathrm{i}}(x) = \frac{z_0\exp(i\kappa z)}{z_0+iz}\exp\left(-\frac{1}{2}\frac{\kappa(x^2+y^2)}{z_0+iz}\right)\begin{pmatrix} \dfrac{ix}{z_0+iz} \\ \dfrac{iy}{z_0+iz} \\ 1-\dfrac{1}{\kappa(z_0+iz)}+\dfrac{1}{2}\dfrac{x^2+y^2}{(z_0+iz)^2} \end{pmatrix}\times\mathbf{p},$$

for any $x = (x, y, z)$, where $z_0 = \frac{\kappa w^2}{2}$ denotes the Rayleigh length. This is an approximate solution of the time-harmonic Maxwell equations assuming that $w \geq \frac{2\lambda}{\pi}$. The reader can refer to [41] for more details.

In Figure 5, we represent cross-sections of the real part of x-component of the different incident electric fields. Thereafter, we investigate the numerical orders of convergence for the

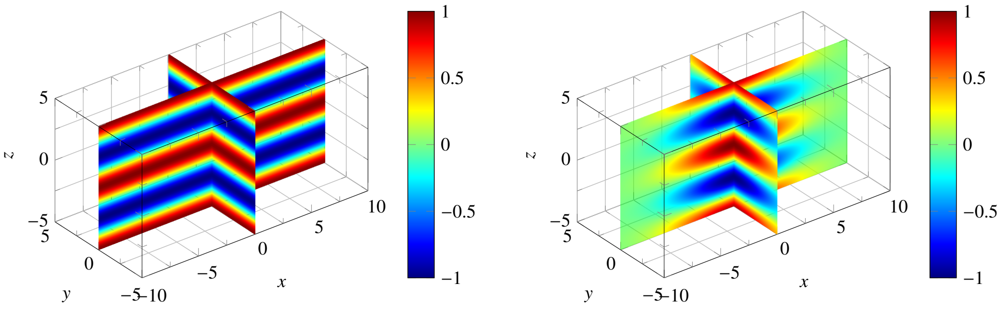

(a) Plane wave

(b) Gaussian beam

Figure 5: Cross sections of real part of the incident electric fields for $\lambda = 5$ and $w = 5$.

outer and inner approximations. The norm used in the comparison is the Sobolev $\mathbf{L}^2$-norm of the difference between the reference solution and the approximate ones, computed into some domains of interest. To obtain the data, we compute

- the reference scattered fields $(\boldsymbol{E}^{\mathrm{s}}_{\delta}, \boldsymbol{H}^{\mathrm{s}}_{\delta})$ from their Mie series representation truncated at $N_{\mathrm{mod}} = 8$, with analytical coefficients[1] for Test 1 and approximate coefficients, computed from projections[2] of the incident field onto the vector spherical harmonics for Test 2,

- the inner approximation $(\widehat{\boldsymbol{E}}_{\delta,P}, \widehat{\boldsymbol{H}}_{\delta,P})$ or the outer approximation $(\widetilde{\boldsymbol{E}}_{\delta,P+3}, \widetilde{\boldsymbol{H}}_{\delta,P+3})$ for $P = 0, 1$ or 2, defined by (A.29)-(A.30),

- the relative errors $\|\boldsymbol{E}^{\mathrm{s}}_{\delta} - \diamond^{\mathrm{E}}\|/\|\boldsymbol{E}^{\mathrm{i}} + \boldsymbol{E}^{\mathrm{s}}_{\delta}\|$ and $\|\boldsymbol{H}^{\mathrm{s}}_{\delta} - \diamond^{\mathrm{H}}\|/\|\boldsymbol{H}^{\mathrm{i}} + \boldsymbol{H}^{\mathrm{s}}_{\delta}\|$, replacing $(\diamond^{\mathrm{E}}, \diamond^{\mathrm{H}})$ either by $(\widehat{\boldsymbol{E}}_{\delta,P}(\cdot/\delta), \widehat{\boldsymbol{H}}_{\delta,P}(\cdot/\delta))$ or $(\widetilde{\boldsymbol{E}}_{\delta,P+3}, \widetilde{\boldsymbol{H}}_{\delta,P+3})$, computed in spherical coordinates by using a Riemann sum for angles θ and φ and a trapezoidal rule for radius r,

for a range of δ between 10^{-4} and 10^{0}. In Figures 6 and 7, we draw cross sections of the modulus of x-component of the electric field induced by the two different tests with $\delta = 0.5$, resp. $\delta = 0.1$.

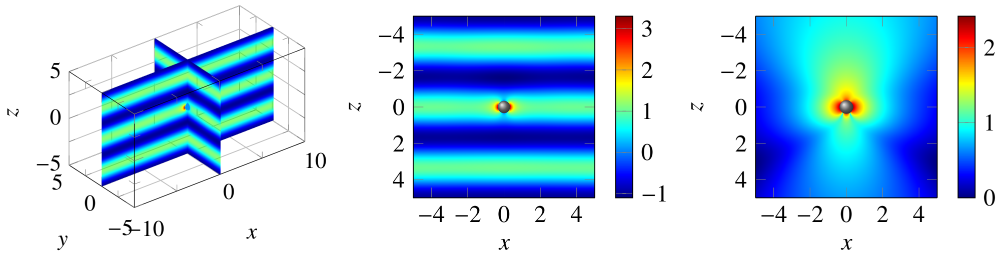

(a) Total electric field (b) Total electric field ($y = 0$) (c) Scattered electric field ($y = 0$)

Figure 6: Cross sections of x-component of the electric field associated to Test 1 with $\lambda = 5$ and $\delta = 0.5$.

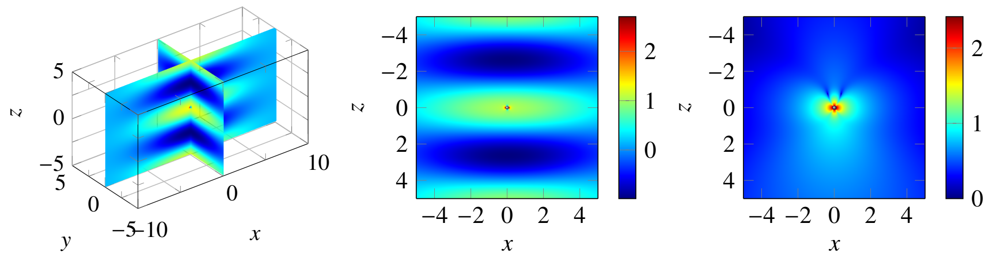

(a) Total electric field (b) Total electric field ($y = 0$) (c) Scattered electric field ($y = 0$)

Figure 7: Cross sections of x-component of the electric field associated to Test 2 with $\lambda = 5$, $w = 5$ and $\delta = 0.1$.

5.2. *Inner approximation*

Let $\Omega^{2\delta}_{\delta}$ be the subdomain of Ω_{δ} independent of δ in the fast variable X, defined by

[1] from the Anger-Jacobi representation [34].

[2] we use a quadrature formula based on the Simpson's rule.

$$x \in \Omega_\delta^{2\delta} = \mathcal{B}(0,2\delta) \setminus \overline{\mathcal{B}(0,\delta)} \qquad \Longleftrightarrow \qquad \mathrm{X} \in \Omega_1^2 = \mathcal{B}(0,2) \setminus \overline{\mathcal{B}(0,1)}$$

For the results in Figures 8 and 9, we investigate the numerical order of convergence in $\mathbf{L}^2(\Omega_1^2)$-norm of the inner approximations with respect to the size of the scatterers δ such that

$$\delta \in \left\{ \frac{1}{10^p},\ p = 0.5 : 0.1 : 3.5 \right\}.$$

Figure 8 depicts the different orders of convergence for the inner approximations $(\widehat{\boldsymbol{E}}_{\delta,P}, \widehat{\boldsymbol{H}}_{\delta,P})$ for $P = 0, 1, 2$, induced by Test 1. The results are consistant in comparison with (A.32). Figure 9

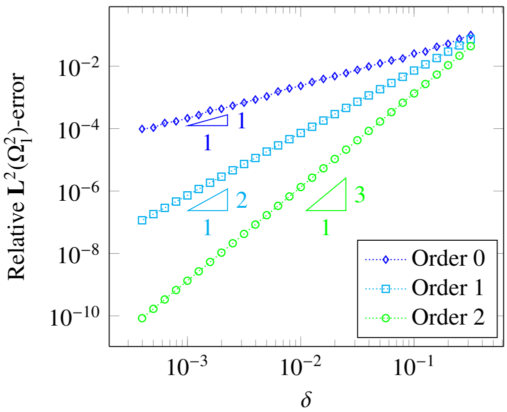

(a) Electric field

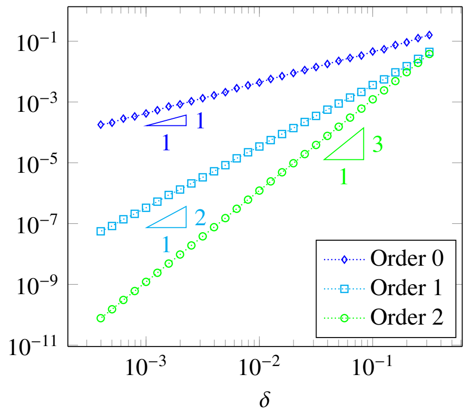

(b) Magnetic field

Figure 8: Relative $\mathbf{L}^2$-errors for the inner approximations associated with Test 1 with $\lambda = 5$ depending on δ.

shows similar results for electric field induced by Test 2. Numerically, we observe that for these three first approximations, the following estimate hold

$$\begin{aligned} \|\boldsymbol{E}_\delta^{\mathrm{s}}(\delta\,\cdot) - \widehat{\boldsymbol{E}}_{\delta,P}\|_{\mathbf{L}^2(\Omega_1^2)} &\le c\,\delta^{P+1} \|\boldsymbol{E}_\delta^{\mathrm{s}}(\delta\,\cdot) + \boldsymbol{E}^{\mathrm{i}}(\delta\,\cdot)\|_{\mathbf{L}^2(\Omega_1^2)}, \\ \|\boldsymbol{H}_\delta^{\mathrm{s}}(\delta\,\cdot) - \widehat{\boldsymbol{H}}_{\delta,P}\|_{\mathbf{L}^2(\Omega_1^2)} &\le c\,\delta^{P+1} \|\boldsymbol{H}_\delta^{\mathrm{s}}(\delta\,\cdot) + \boldsymbol{H}^{\mathrm{i}}(\delta\,\cdot)\|_{\mathbf{L}^2(\Omega_1^2)}. \end{aligned}$$

The convergence of the inner asymptotics is numerically validated regarding error estimates (A.32). For the results of Test 2, a loss of convergence in asymptotic regime is due to the approximation of the incident gaussian beam.

5.3. *Outer approximation*

Let $\Omega_\lambda^{2\lambda}$ be the subdomain of Ω_δ independent of δ given by

$$\Omega_\lambda^{2\lambda} = \mathcal{B}(0,2\lambda) \setminus \overline{\mathcal{B}(0,\lambda)}.$$

For the results in Figures 10 and 11, we investigate the numerical order of convergence for $\mathbf{L}^2(\Omega_\lambda^{2\lambda})$-norm of the outer approximations with respect to the size δ of the obstacles such that

$$\delta \in \left\{ \frac{1}{10^p},\ p = 0.3 : 0.1 : 3.2 \right\}.$$

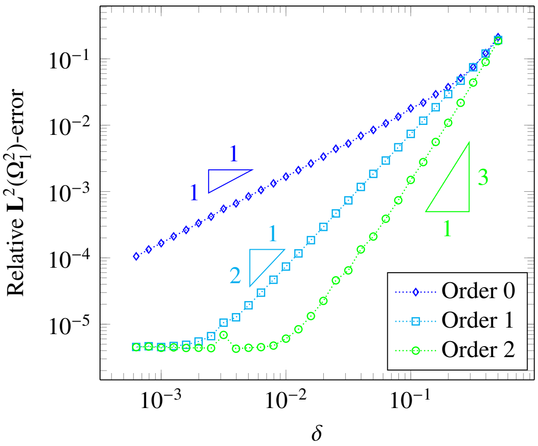

Figure 9: Relative $\mathbf{L}^2$-errors for the inner electric approximations associated with Test 2 with $\lambda = 5$ and $w = 5$ depending on δ.

Figure 10 displays the different orders of convergence for the outer approximations $(\widetilde{\boldsymbol{E}}_{\delta,3}, \widetilde{\boldsymbol{H}}_{\delta,3})$, $(\widetilde{\boldsymbol{E}}_{\delta,5}, \widetilde{\boldsymbol{H}}_{\delta,5})$ and the collected dipolar model, see Paragraph 4.1, induced by Test 1, using $\mathbf{L}^2$-norm into $\Omega_\lambda^{2\lambda}$. Figure 11 shows similar results for the outer approximations of the electric field

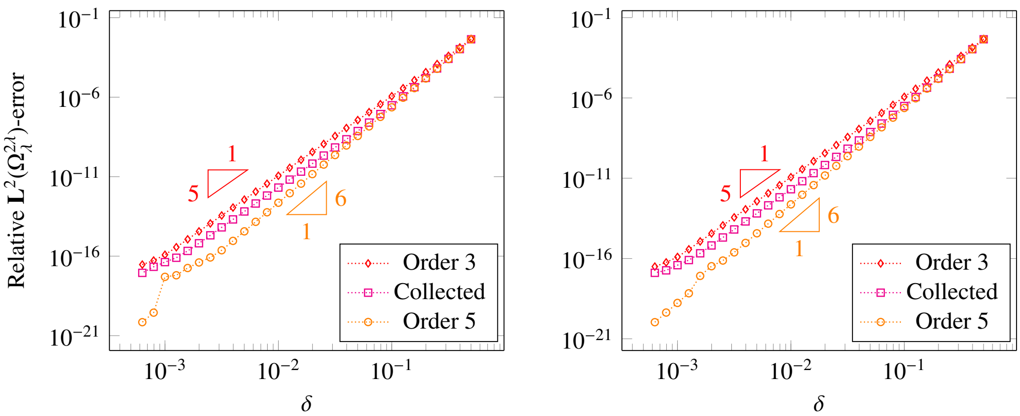

(a) Electric field

(b) Magnetic field

Figure 10: Relative $\mathbf{L}^2$-errors for the outer approximations associated to Test 1 with $\lambda = 5$ depending on δ.

induced by Test 2. Except the collected approximation, noting that the fourth-order outer term is identically zero, we observe that for the first outer approximations, the following estimate holds

$$\|\boldsymbol{E}_\delta^{\mathrm{s}} - \widetilde{\boldsymbol{E}}_{\delta,P}\|_{\mathbf{L}^2(\Omega_\lambda^{2\lambda})} \leq c\, \delta^{P+1} \|\boldsymbol{E}_\delta^{\mathrm{s}} + \boldsymbol{E}^{\mathrm{i}}\|_{\mathbf{L}^2(\Omega_\lambda^{2\lambda})}, \qquad \|\boldsymbol{H}_\delta^{\mathrm{s}} - \widetilde{\boldsymbol{H}}_{\delta,P}\|_{\mathbf{L}^2(\Omega_\lambda^{2\lambda})} \leq c\, \delta^{P+1} \|\boldsymbol{H}_\delta^{\mathrm{s}} + \boldsymbol{H}^{\mathrm{i}}\|_{\mathbf{L}^2(\Omega_\lambda^{2\lambda})}.$$

The convergence of outer asymptotics is numerically validated regarding error estimates (A.31). For the results of Test 1, the different orders of convergence are consistant in comparison with

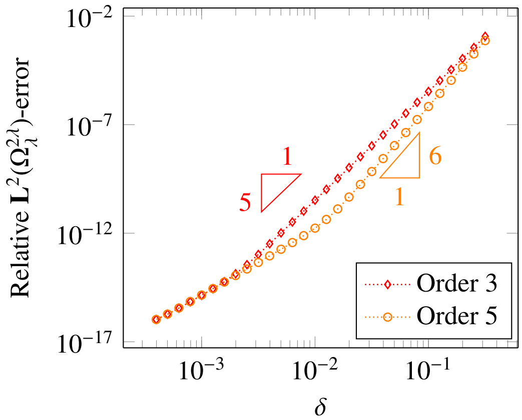

Figure 11: Relative $\mathbf{L}^2$-errors for the outer approximations associated to Test 2 with $\lambda = 5$ and $w = 5$ depending on δ.

(A.31). For the results of Test 2, a loss of convergence in asymptotic regime is due to the approximation of the incident gaussian beam.

6. Conclusion and perspectives

The asymptotic analysis has turned out to be very relevant and efficient to derive approximate solutions of the electromagnetic wave scattering problem by a small obstacle. Local approximations of electromagnetic fields have been derived and made explicit for a spherical scatterer thanks to the matched asymptotic expansion method. The method provides accurate approximations as it is shown by numerical tests, while allowing the size of the obstacles to be very small compared to the incident wavelength. Being analytic, the implementation is very simple and the computational cost is very low.

Multiple scattering. This work is a first step to consider the multiple scattering problem by spherical obstacles. In contrast with the Born approximation, the Foldy theory suggests to take into consideration interactions between the scaterrers by approximating the scattered field as the superposition of scattered fields generated by dipoles whose dipolar moments take into account the local scattered fields as an incident wave for the other scatterers. Spectral-based methods have been also developed to tackle multiple scattering problems in electromagnetism, see for instance [42, 9, 43]. Comparisons between a such method and asymptotic models for multiple scattering will be subject of a further work.

General geometry. A coupling between asymptotic models and a numerical method is required to take into account obstacles of arbitary shape. Indeed, for a general geometry, inner problems cannot be solved by the technique of separation of variables and the multipolar moments have to be approximated.

Time-dependent domain. The application of the inverse Fourier transform should allow to deduce properties for the time-dependent problem. In particular, the identification of time-harmonic symbol $(-i\omega)$ with partial time-derivative ∂_t has been already explored for the wave equation [21] in contrast with the Helmholtz equation [23].

Appendix A. The matched asymptotic expansions

In this section, we develop the method of matched asymptotic expansions [14, 15] for solving the exterior time-harmonic Maxwell problem (2.1). This method involves two different approximations, the so-called *outer* and *inner* expansions. The outer expansion approximates the solution far from the obstacle and it is defined into the punctured domain

$$\Omega^\star = \mathbb{R}^3 \setminus \{0\}.$$

The inner expansion approximates the solution close to the obstacle and is defined in fast variable X into the scaled domain

$$\widehat{\Omega} = \mathbb{R}^3 \setminus \overline{\mathcal{B}(0,1)}.$$

We present the global construction of the asymptotic expansions including problems satisfied by the successive terms, and how the expansions are related thanks to a matching procedure. Finally, we apply the algorithm for deriving the first terms of the expansions.

Appendix A.1. Equations for the coefficients of the outer expansion

Far from the obstacle, the exact solution is approximated by the outer expansion

$$\boldsymbol{E}_\delta(x) \underset{\delta\to 0}{\sim} \sum_{p=0}^{\infty} \delta^p \widetilde{\boldsymbol{E}}_p(x), \qquad \boldsymbol{H}_\delta(x) \underset{\delta\to 0}{\sim} \sum_{p=0}^{\infty} \delta^p \widetilde{\boldsymbol{H}}_p(x), \tag{A.1}$$

where $x = r\widehat{x}$ is the space variable. The terms $(\widetilde{\boldsymbol{E}}_p, \widetilde{\boldsymbol{H}}_p)$, have to satisfy, for any $p \geq 0$,

$$\begin{cases} \nabla \times \widetilde{\boldsymbol{E}}_p - i\kappa \widetilde{\boldsymbol{H}}_p = 0 & \text{in } \Omega^\star, \\ \nabla \times \widetilde{\boldsymbol{H}}_p + i\kappa \widetilde{\boldsymbol{E}}_p = 0 & \text{in } \Omega^\star, \\ \lim\limits_{r\to\infty} r(\widetilde{\boldsymbol{H}}_p \times \widehat{x} - \widetilde{\boldsymbol{E}}_p) = 0 & \text{uniformly in } \widehat{x}. \end{cases} \tag{A.2}$$

These problems are obtained by inserting the asymptotic expansions (A.1) into (2.1) and by identifying the terms with the same powers in δ. To alter the ill-posedness of these problems in $\mathbf{H}_{\mathrm{loc}}(\nabla\times, \Omega^\star)$, the space of vector fields $\boldsymbol{u}$ such that

$$\forall \chi \in \mathscr{C}_c^\infty(\mathbb{R}^3),\ \chi = 0 \text{ in a neighborhood of } 0, \qquad \chi\boldsymbol{u} \in \mathbf{L}^2(\mathbb{R}^3) \text{ and } \nabla \times (\chi\boldsymbol{u}) \in \mathbf{L}^2(\mathbb{R}^3),$$

the behavior of $(\widetilde{\boldsymbol{E}}_p, \widetilde{\boldsymbol{H}}_p)$ in the vicinity of the origin is required and will be given by the matching conditions (A.12).

Appendix A.2. Equations for coefficients of the inner expansion

In a neighborhood of the obstacle, the solution is approximated by the inner expansion

$$\boldsymbol{E}_\delta(\delta \mathrm{X}) \underset{\delta\to 0}{\sim} \sum_{p=0}^{\infty} \delta^p \widehat{\boldsymbol{E}}_p(\mathrm{X}), \qquad \boldsymbol{H}_\delta(\delta \mathrm{X}) \underset{\delta\to 0}{\sim} \sum_{p=0}^{\infty} \delta^p \widehat{\boldsymbol{H}}_p(\mathrm{X}), \tag{A.3}$$

where $\mathrm{X} = \delta^{-1}x = \mathrm{R}\widehat{x}$ denotes the fast variable. To obtain the equations satisfied by the terms $(\widehat{\boldsymbol{E}}_p, \widehat{\boldsymbol{H}}_p)$, we make the scaling $\mathrm{X} = \delta^{-1}x$ into the curl operator ($\delta^{-1}\nabla_{\mathrm{X}} \times \boldsymbol{u} = \nabla_x \times \boldsymbol{u}$) and we insert the expansions (A.3) into the volumic equations (2.1). The inner expansions then satisfy

$$\begin{cases} \dfrac{1}{\delta}\nabla_{\mathrm{X}} \times \displaystyle\sum_{p=0}^{\infty} \delta^p \widehat{\boldsymbol{E}}_p - i\kappa \sum_{p=0}^{\infty} \delta^p \widehat{\boldsymbol{H}}_p = 0 & \text{in } \widehat{\Omega}, \\ \dfrac{1}{\delta}\nabla_{\mathrm{X}} \times \displaystyle\sum_{p=0}^{\infty} \delta^p \widehat{\boldsymbol{H}}_p + i\kappa \sum_{p=0}^{\infty} \delta^p \widehat{\boldsymbol{E}}_p = 0 & \text{in } \widehat{\Omega}. \end{cases}$$

We perform in these equations the identification of terms with the same power of δ. We thus see that, since $\kappa \neq 0$, the terms $(\widehat{\boldsymbol{E}}_p, \widehat{\boldsymbol{H}}_p)$ have to satisfy, for any $p \geq 0$, the uncoupled nested Maxwell equations,

$$\begin{cases} \nabla \times \widehat{\boldsymbol{E}}_p = i\kappa \widehat{\boldsymbol{H}}_{p-1} & \text{in } \widehat{\Omega}, \\ \nabla \cdot \widehat{\boldsymbol{E}}_p = 0 & \text{in } \widehat{\Omega}, \end{cases} \qquad \begin{cases} \nabla \times \widehat{\boldsymbol{H}}_p = -i\kappa \widehat{\boldsymbol{E}}_{p-1} & \text{in } \widehat{\Omega}, \\ \nabla \cdot \widehat{\boldsymbol{H}}_p = 0 & \text{in } \widehat{\Omega}, \end{cases} \tag{A.4}$$

using the convention $\widehat{\boldsymbol{E}}_{-1} = \widehat{\boldsymbol{H}}_{-1} = 0$. The boundary conditions on $\widehat{\Gamma} := \partial\widehat{\Omega}$ are obtained by identifying the Taylor series expansion in fast variable of the incident field in a neighborhood of the origin and the boundary conditions satisfied by the exact solution on $\partial\Omega_\delta$, with respect to the powers in δ. We have

$$\begin{cases} \mathbf{n} \times \widehat{\boldsymbol{E}}_p = -\mathbf{n} \times \widehat{\boldsymbol{E}}^{\mathrm{i}}_p & \text{on } \widehat{\Gamma}, \\ \mathbf{n} \cdot \widehat{\boldsymbol{H}}_p = -\mathbf{n} \cdot \widehat{\boldsymbol{H}}^{\mathrm{i}}_p & \text{on } \widehat{\Gamma}, \end{cases} \tag{A.5}$$

where

$$\widehat{\boldsymbol{E}}^{\mathrm{i}}_p(\mathrm{X}) = \sum_{|\alpha|=p} \frac{1}{\alpha!} D^\alpha \boldsymbol{E}^{\mathrm{i}}(0)(\mathrm{X}^\alpha), \qquad \widehat{\boldsymbol{H}}^{\mathrm{i}}_p(\mathrm{X}) = \sum_{|\alpha|=p} \frac{1}{\alpha!} D^\alpha \boldsymbol{H}^{\mathrm{i}}(0)(\mathrm{X}^\alpha).$$

The inner problems will be solved by induction for $p \geq 0$. To do that, we decompose the successive terms $(\widehat{\boldsymbol{E}}_p, \widehat{\boldsymbol{H}}_p)$ as the sum of $p+1$ vector fields

$$\widehat{\boldsymbol{E}}_p(\mathrm{X}) = \sum_{\ell=0}^{p} \widehat{\boldsymbol{E}}_{p,\ell}(\mathrm{X}), \qquad \widehat{\boldsymbol{H}}_p(\mathrm{X}) = \sum_{\ell=0}^{p} \widehat{\boldsymbol{H}}_{p,\ell}(\mathrm{X}). \tag{A.6}$$

For $\ell = 0, \dots, p$, the terms $(\widehat{\boldsymbol{E}}_{p,\ell}, \widehat{\boldsymbol{H}}_{p,\ell})$ have to satisfy the following nested equations

$$\begin{cases} \nabla \times \widehat{\boldsymbol{E}}_{p,\ell} = i\kappa \widehat{\boldsymbol{H}}_{p-1,\ell-1} & \text{in } \widehat{\Omega}, \\ \nabla \cdot \widehat{\boldsymbol{E}}_{p,\ell} = 0 & \text{in } \widehat{\Omega}, \end{cases} \qquad \begin{cases} \nabla \times \widehat{\boldsymbol{H}}_{p,\ell} = -i\kappa \widehat{\boldsymbol{E}}_{p-1,\ell-1} & \text{in } \widehat{\Omega}, \\ \nabla \cdot \widehat{\boldsymbol{H}}_{p,\ell} = 0 & \text{in } \widehat{\Omega}, \end{cases} \tag{A.7}$$

using the convention $\widehat{\boldsymbol{E}}_{p,-1} = \widehat{\boldsymbol{H}}_{p,-1} = 0$ for any integer p. To compute the inner terms of order $p \geq 0$, we have firstly to determine particular solutions of (A.7) for $\ell = 1, \dots, p$ and then, to solve quasi-static problems satisfied by the header terms $\widehat{\boldsymbol{E}}_{p,0}$ and $\widehat{\boldsymbol{H}}_{p,0}$ in $\mathbf{L}^2(\widehat{\Omega})$. It is worth noting that additional conditions are required to guarantee the uniqueness of the electric terms,

$$\int_{\widehat{\Gamma}} \mathbf{n} \cdot \widehat{\boldsymbol{E}}_p \, ds = 0, \qquad \text{for any } p \geq 0. \tag{A.8}$$

These null-charge conditions, called *gauge conditions* in [44, 45, 46], occur when $\kappa \neq 0$ and are deduced from the initial problem (2.1),

$$-i\kappa \int_{\Gamma_\delta} \mathbf{n} \cdot \boldsymbol{E}_\delta \, ds = \int_{\Gamma_\delta} (\nabla \times \boldsymbol{H}_\delta) \cdot \mathbf{n} \, ds = \int_{\Gamma_\delta} \operatorname{curl}_{\Gamma_\delta} [\mathbf{n} \times (\boldsymbol{H}_\delta \times \mathbf{n})] \, ds = 0. \tag{A.9}$$

The last equality is obtained from the Stokes identity [35]. Conditions (A.8) are then obtained by inserting the asymptotic expansion (A.3) into (A.9) and by identifying with the same powers in δ.

Appendix A.3. Matching conditions

The outer and inner expansions are related thanks to a matching procedure which allows to determine the behavior of $(\widetilde{\boldsymbol{E}}_p, \widetilde{\boldsymbol{H}}_p)$ close to the origin and the behavior of $(\widehat{\boldsymbol{E}}_p, \widehat{\boldsymbol{H}}_p)$ towards the infinity. For $p \geq 0$, we expand $\widetilde{\boldsymbol{E}}_p$ and $\widetilde{\boldsymbol{H}}_p$ in a neighborhood of the origin,

$$\widetilde{\boldsymbol{E}}_p(r\widehat{x}) \underset{r\to 0}{\sim} \sum_{q=-\infty}^{+\infty} (\kappa r)^q \widetilde{\boldsymbol{E}}_p^q(\widehat{x}), \qquad \widetilde{\boldsymbol{H}}_p(r\widehat{x}) \underset{r\to 0}{\sim} \sum_{q=-\infty}^{+\infty} (\kappa r)^q \widetilde{\boldsymbol{H}}_p^q(\widehat{x}) \tag{A.10}$$

and $\widehat{\boldsymbol{E}}_p$ and $\widehat{\boldsymbol{H}}_p$ towards the infinity, in the fast variable $\mathrm{X} = \mathrm{R}\widehat{x}$,

$$\widehat{\boldsymbol{E}}_p(\mathrm{R}\widehat{x}) \underset{\mathrm{R}\to +\infty}{\sim} \sum_{q=-\infty}^{+\infty} (\kappa \mathrm{R})^q \widehat{\boldsymbol{E}}_p^q(\widehat{x}), \qquad \widehat{\boldsymbol{H}}_p(\mathrm{R}\widehat{x}) \underset{\mathrm{R}\to +\infty}{\sim} \sum_{q=-\infty}^{+\infty} (\kappa \mathrm{R})^q \widehat{\boldsymbol{H}}_p^q(\widehat{x}). \tag{A.11}$$

We will call *singular* part of the outer terms $(\widetilde{\boldsymbol{E}}_p, \widetilde{\boldsymbol{H}}_p)$ the series expansions

$$\sum_{q<0} (\kappa r)^q \widetilde{\boldsymbol{E}}_p^q(\widehat{x}), \qquad \sum_{q<0} (\kappa r)^q \widetilde{\boldsymbol{H}}_p^q(\widehat{x}).$$

In the previous series expansions, it appears a singularity at the origin due to the negative powers of r. The *regular* part is naturally defined by the series with non-negative indices q. In addition, we define the *increasing* part of the inner expansion by

$$\sum_{q\geq 0} (\kappa \mathrm{R})^q \widehat{\boldsymbol{E}}_p^q(\widehat{x}), \qquad \sum_{q\geq 0} (\kappa \mathrm{R})^q \widehat{\boldsymbol{H}}_p^q(\widehat{x}).$$

and reciprocally the *decreasing* part, with indices $q < 0$. Following [14], the expansions (A.1) and (A.3) are matched in the overlapping area by using the expansions (A.10) and (A.11) and by identifying the terms with the same powers of δ and κr. We differentiate two matching formulations following the sign of $q \in \mathbb{R}$,

$$\begin{cases} (\widetilde{\boldsymbol{E}}_p^q, \widetilde{\boldsymbol{H}}_p^q) = (\widehat{\boldsymbol{E}}_{p+q}^q, \widehat{\boldsymbol{H}}_{p+q}^q), & -p \leq q < 0, \\ (\widetilde{\boldsymbol{E}}_p^q, \widetilde{\boldsymbol{H}}_p^q) = 0, & p \leq 0 \text{ or } q < -p, \end{cases} \tag{A.12}$$

and

$$\begin{cases} (\widehat{\boldsymbol{E}}_p^q, \widehat{\boldsymbol{H}}_p^q) = (\widetilde{\boldsymbol{E}}_{p-q}^q, \widetilde{\boldsymbol{H}}_{p-q}^q), & 0 \leq q \leq p, \\ (\widehat{\boldsymbol{E}}_p^q, \widehat{\boldsymbol{H}}_p^q) = 0, & p < 0 \text{ or } q > p. \end{cases} \tag{A.13}$$

As a result, the singular part of the outer terms is linked with the decreasing part of the inner terms and the increasing part of the inner terms is linked with the regular part of the outer terms.

Remark 8. In spherical geometries, modal decomposition of solutions can be used to determine angular terms $(\widetilde{\boldsymbol{E}}_p^q, \widetilde{\boldsymbol{H}}_p^q)$ and $(\widehat{\boldsymbol{E}}_p^q, \widehat{\boldsymbol{H}}_p^q)$ and to make explicit the matching conditions (A.12)-(A.13) through the spectral coefficients, see [33, Proposition 1].

Appendix A.4. Algorithm of construction

In this paragraph, we present the algorithm of construction of successive terms of the asymptotic expansions. Let p be a non-negative integer. Assuming that all the terms $(\widetilde{\boldsymbol{E}}_k, \widetilde{\boldsymbol{H}}_k)$ and $(\widehat{\boldsymbol{E}}_k, \widehat{\boldsymbol{H}}_k)$ are known up to the order $p-1$, we show how to derive the inner and outer terms of order p. This algorithm can be divided in two parts. On the one hand, the matching conditions (A.12) allow to derive the singular part of the outer terms $(\widetilde{\boldsymbol{E}}_p, \widetilde{\boldsymbol{H}}_p)$. The regular part is then given by solving (A.2) in $\mathbb{R}^3$, which is identically zero because of the Silver-Müller radiation condition. On the other hand, the matching conditions (A.13) clarify the behavior towards the infinity of the inner terms $(\widehat{\boldsymbol{E}}_p, \widehat{\boldsymbol{H}}_p)$. These latter are then determined by solving the nested problems (A.4) equipped with the boundary conditions (A.5) and the null-charge condition (A.8) for the electric terms. To summarize, the terms of order p into the asymptotic expansions are derived by solving successively

$$
\left\{
\begin{array}{lrl}
\left.\begin{array}{ll}
(\widetilde{\boldsymbol{E}}_p^q, \widetilde{\boldsymbol{H}}_p^q) = (\widehat{\boldsymbol{E}}_{p+q}^q, \widehat{\boldsymbol{H}}_{p+q}^q), & -p \le q < 0, \\
(\widetilde{\boldsymbol{E}}_p^q, \widetilde{\boldsymbol{H}}_p^q) = 0, & p \le 0 \text{ or } q < -p,
\end{array}\right\} & & \textit{(i)} \\
\left.\begin{array}{ll}
\nabla \times \widetilde{\boldsymbol{E}}_p - i\kappa \widetilde{\boldsymbol{H}}_p = 0 & \text{in } \Omega^\star, \\
\nabla \times \widetilde{\boldsymbol{H}}_p + i\kappa \widetilde{\boldsymbol{E}}_p = 0 & \text{in } \Omega^\star, \\
\lim\limits_{r\to\infty} r(\widetilde{\boldsymbol{H}}_p \times \widehat{x} - \widetilde{\boldsymbol{E}}_p) = 0 & \text{uniformly in } \widehat{x},
\end{array}\right\} & & \textit{(ii)} \\
\left.\begin{array}{ll}
(\widehat{\boldsymbol{E}}_p^q, \widehat{\boldsymbol{H}}_p^q) = (\widetilde{\boldsymbol{E}}_{p-q}^q, \widetilde{\boldsymbol{H}}_{p-q}^q), & 0 \le q \le p, \\
(\widehat{\boldsymbol{E}}_p^q, \widehat{\boldsymbol{H}}_p^q) = 0, & p < 0 \text{ or } q > p.
\end{array}\right\} & & \textit{(iii)} \\
\left.\begin{array}{ll}
\nabla \times \widehat{\boldsymbol{E}}_p = i\kappa \widehat{\boldsymbol{H}}_{p-1} & \text{in } \widehat{\Omega}, \\
\nabla \cdot \widehat{\boldsymbol{E}}_p = 0 & \text{in } \widehat{\Omega}, \\
\mathbf{n} \times \widehat{\boldsymbol{E}}_p = -\mathbf{n} \times \widehat{\boldsymbol{E}}_p^{\mathrm{i}} & \text{on } \widehat{\Gamma}, \\
\displaystyle\int_{\widehat{\Gamma}} \mathbf{n} \cdot \widehat{\boldsymbol{E}}_p \, ds = 0, &
\end{array}\right\} & & \textit{(iv)} \\
\left.\begin{array}{ll}
\nabla \times \widehat{\boldsymbol{H}}_p = -i\kappa \widehat{\boldsymbol{E}}_{p-1} & \text{in } \widehat{\Omega}, \\
\nabla \cdot \widehat{\boldsymbol{H}}_p = 0 & \text{in } \widehat{\Omega}, \\
\mathbf{n} \cdot \widehat{\boldsymbol{H}}_p = -\mathbf{n} \cdot \widehat{\boldsymbol{H}}_p^{\mathrm{i}} & \text{on } \widehat{\Gamma}.
\end{array}\right\} & & \textit{(v)}
\end{array}
\right. \tag{A.14}
$$

Appendix A.5. First terms of the asymptotics

Step $p = 0$. Equations *(i)* of (A.14) imply that the zeroth-order outer terms $(\widetilde{\boldsymbol{E}}_0, \widetilde{\boldsymbol{H}}_0)$ do not possess singularity at the origin. Since they satisfy the Silver-Müller radiation condition at infinity, see *(ii)* of (A.14), $(\widetilde{\boldsymbol{E}}_0, \widetilde{\boldsymbol{H}}_0)$ are identically zero. According to *(iii)* of (A.14), the behavior towards the infinity of the inner terms of order 0 is given by

$$
\widehat{\boldsymbol{E}}_0 = \underset{\mathrm{R}\to\infty}{O}(\mathrm{R}^{-1}) \qquad \text{and} \qquad \widehat{\boldsymbol{H}}_0 = \underset{\mathrm{R}\to\infty}{O}(\mathrm{R}^{-1}).
$$

Hence, according to *(iv)-(v)* of (A.14), the zeroth-order terms $\widehat{\boldsymbol{E}}_0$ and $\widehat{\boldsymbol{H}}_0$ solve the following problems,

$$\begin{cases} \nabla\times\widehat{\boldsymbol{E}}_0 = 0 & \text{in } \widehat{\Omega}, \\ \nabla\cdot\widehat{\boldsymbol{E}}_0 = 0 & \text{in } \widehat{\Omega}, \\ \mathbf{n}\times\widehat{\boldsymbol{E}}_0 = -\mathbf{n}\times\boldsymbol{E}^{\mathrm{i}}(0) & \text{on } \widehat{\Gamma}, \\ \widehat{\boldsymbol{E}}_0 = \underset{\mathrm{R}\to\infty}{O}(\mathrm{R}^{-1}) & \text{at infinity}, \\ \displaystyle\int_{\widehat{\Gamma}} \mathbf{n}\cdot\widehat{\boldsymbol{E}}_0\, ds = 0, \end{cases} \qquad \begin{cases} \nabla\times\widehat{\boldsymbol{H}}_0 = 0 & \text{in } \widehat{\Omega}, \\ \nabla\cdot\widehat{\boldsymbol{H}}_0 = 0 & \text{in } \widehat{\Omega}, \\ \mathbf{n}\cdot\widehat{\boldsymbol{H}}_0 = -\mathbf{n}\cdot\boldsymbol{H}^{\mathrm{i}}(0) & \text{on } \widehat{\Gamma}, \\ \widehat{\boldsymbol{H}}_0 = \underset{\mathrm{R}\to\infty}{O}(\mathrm{R}^{-1}) & \text{at infinity}. \end{cases} \tag{A.15}$$

These problems can be solved with the technique of separation of variables, see [35, Section 2.5] for solutions to Laplace equation in spherical geometries or [33, Section C.3] for a more adapted framework to nested Maxwell equations. The unique solutions of (A.15) are given by (2.6). In addition, we observe that

$$\widehat{\boldsymbol{E}}_0 = \underset{\mathrm{R}\to\infty}{O}(\mathrm{R}^{-3}) \qquad \text{and} \qquad \widehat{\boldsymbol{H}}_0 = \underset{\mathrm{R}\to\infty}{O}(\mathrm{R}^{-3}). \tag{A.16}$$

Step $p = 1$. Equations *(i)* of (A.14) and (A.16) imply $(\widetilde{\boldsymbol{E}}_1^q, \widetilde{\boldsymbol{H}}_1^q) = (0,0)$ for any $q < 0$. Hence, according to *(ii)* of (A.14), we deduce that

$$\widetilde{\boldsymbol{E}}_1 = \widetilde{\boldsymbol{H}}_1 = 0.$$

Equations *(iii)* of (A.14) imply $(\widehat{\boldsymbol{E}}_1^q, \widehat{\boldsymbol{H}}_1^q) = (0,0)$ for any $q \geq 0$. Hence,

$$\widehat{\boldsymbol{E}}_1 = \underset{\mathrm{R}\to\infty}{O}(\mathrm{R}^{-1}) \qquad \text{and} \qquad \widehat{\boldsymbol{H}}_1 = \underset{\mathrm{R}\to\infty}{O}(\mathrm{R}^{-1}). \tag{A.17}$$

According to (A.17) and *(iv)-(v)* of (A.14), the first-order terms $\widehat{\boldsymbol{E}}_1$ and $\widehat{\boldsymbol{H}}_1$ solve the following nested Maxwell problems,

$$\begin{cases} \nabla\times\widehat{\boldsymbol{E}}_1 = i\kappa\widehat{\boldsymbol{H}}_0 & \text{in } \widehat{\Omega}, \\ \nabla\cdot\widehat{\boldsymbol{E}}_1 = 0 & \text{in } \widehat{\Omega}, \\ \mathbf{n}\times\widehat{\boldsymbol{E}}_1 = -\mathbf{n}\times(\mathbb{J}_{\boldsymbol{E}^{\mathrm{i}}}(0)\widehat{x}) & \text{on } \widehat{\Gamma}, \\ \widehat{\boldsymbol{E}}_1 = \underset{\mathrm{R}\to\infty}{O}(\mathrm{R}^{-1}) & \text{at infinity}, \\ \displaystyle\int_{\widehat{\Gamma}} \mathbf{n}\cdot\widehat{\boldsymbol{E}}_1\, ds = 0, \end{cases} \qquad \begin{cases} \nabla\times\widehat{\boldsymbol{H}}_1 = -i\kappa\widehat{\boldsymbol{E}}_0 & \text{in } \widehat{\Omega}, \\ \nabla\cdot\widehat{\boldsymbol{H}}_1 = 0 & \text{in } \widehat{\Omega}, \\ \mathbf{n}\cdot\widehat{\boldsymbol{H}}_1 = -\mathbf{n}\cdot(\mathbb{J}_{\boldsymbol{H}^{\mathrm{i}}}(0)\widehat{x}) & \text{on } \widehat{\Gamma}, \\ \widehat{\boldsymbol{H}}_1 = \underset{\mathrm{R}\to\infty}{O}(\mathrm{R}^{-1}) & \text{at infinity}. \end{cases}$$

According to (A.6), we decompose the vector fields $\widehat{\boldsymbol{E}}_1$ and $\widehat{\boldsymbol{H}}_1$ under the form

$$\widehat{\boldsymbol{E}}_1 = \widehat{\boldsymbol{E}}_{1,0} + \widehat{\boldsymbol{E}}_{1,1} \qquad \text{and} \qquad \widehat{\boldsymbol{H}}_1 = \widehat{\boldsymbol{H}}_{1,0} + \widehat{\boldsymbol{H}}_{1,1},$$

where $\widehat{\boldsymbol{E}}_{1,1}$ and $\widehat{\boldsymbol{H}}_{1,1}$ are particular solutions of the nested equations obtained by taking $p = \ell = 1$ into (A.7),

$$\begin{cases} \nabla\times\widehat{\boldsymbol{E}}_{1,1} = i\kappa\widehat{\boldsymbol{H}}_0 & \text{in } \widehat{\Omega}, \\ \nabla\cdot\widehat{\boldsymbol{E}}_{1,1} = 0 & \text{in } \widehat{\Omega}, \\ \widehat{\boldsymbol{E}}_{1,1} = \underset{\mathrm{R}\to\infty}{O}(\mathrm{R}^{-1}) & \text{at infinity}, \end{cases} \qquad \begin{cases} \nabla\times\widehat{\boldsymbol{H}}_{1,1} = -i\kappa\widehat{\boldsymbol{E}}_0 & \text{in } \widehat{\Omega}, \\ \nabla\cdot\widehat{\boldsymbol{H}}_{1,1} = 0 & \text{in } \widehat{\Omega}, \\ \widehat{\boldsymbol{H}}_{1,1} = \underset{\mathrm{R}\to\infty}{O}(\mathrm{R}^{-1}) & \text{at infinity}. \end{cases} \tag{A.18}$$

The terms $\widehat{\boldsymbol{E}}_{1,0}$ and $\widehat{\boldsymbol{H}}_{1,0}$ solve the static Maxwell problems obtained by taking $p = 1$ and $\ell = 0$ into (A.7) by taking into account the boundary conditions (A.5) and the condition (A.8),

$$\begin{cases} \nabla \times \widehat{\boldsymbol{E}}_{1,0} = 0 & \text{in } \widehat{\Omega}, \\ \nabla \cdot \widehat{\boldsymbol{E}}_{1,0} = 0 & \text{in } \widehat{\Omega}, \\ \mathbf{n} \times \widehat{\boldsymbol{E}}_{1,0} = -\mathbf{n} \times (\mathbb{J}_{\boldsymbol{E}^{\mathrm{i}}}(0)\widehat{x}) - \mathbf{n} \times \widehat{\boldsymbol{E}}_{1,1} & \text{on } \widehat{\Gamma}, \\ \widehat{\boldsymbol{E}}_{1,0} = \underset{\mathrm{R}\to\infty}{O}(\mathrm{R}^{-1}) & \text{at infinity}, \\ \displaystyle\int_{\widehat{\Gamma}} \mathbf{n} \cdot \widehat{\boldsymbol{E}}_{1,0}\, ds = -\int_{\widehat{\Gamma}} \mathbf{n} \cdot \widehat{\boldsymbol{E}}_{1,1}, \end{cases} \tag{A.19}$$

and

$$\begin{cases} \nabla \times \widehat{\boldsymbol{H}}_{1,0} = 0 & \text{in } \widehat{\Omega}, \\ \nabla \cdot \widehat{\boldsymbol{H}}_{1,0} = 0 & \text{in } \widehat{\Omega}, \\ \mathbf{n} \cdot \widehat{\boldsymbol{H}}_{1,0} = -\mathbf{n} \cdot (\mathbb{J}_{\boldsymbol{H}^{\mathrm{i}}}(0)\widehat{x}) - \mathbf{n} \cdot \widehat{\boldsymbol{H}}_{1,1} & \text{on } \widehat{\Gamma}, \\ \widehat{\boldsymbol{H}}_{1,0} = \underset{\mathrm{R}\to\infty}{O}(\mathrm{R}^{-1}) & \text{at infinity}. \end{cases} \tag{A.20}$$

These problems are solved with the technique of separation of variables. Particular solutions of (A.18) are given by

$$\widehat{\boldsymbol{E}}_{1,1}(\mathrm{X}) = \frac{i\kappa}{2\mathrm{R}^2}\gamma_\times[\boldsymbol{H}^{\mathrm{i}}(0)], \qquad \widehat{\boldsymbol{H}}_{1,1}(\mathrm{X}) = \frac{i\kappa}{\mathrm{R}^2}\gamma_\times[\boldsymbol{E}^{\mathrm{i}}(0)], \qquad \mathrm{X} \in \widehat{\Omega}. \tag{A.21}$$

The boundary conditions into (A.19) and (A.20) can be written as

$$\mathbf{n} \times \widehat{\boldsymbol{E}}_{1,0} = -\mathbf{n} \times \left(\mathbb{J}^{\mathrm{s}}_{\boldsymbol{E}^{\mathrm{i}}}(0)\widehat{x}\right) \qquad \text{and} \qquad \mathbf{n} \cdot \widehat{\boldsymbol{H}}_{1,0} = \mathbf{n} \cdot (\mathbb{J}_{\boldsymbol{H}^{\mathrm{i}}}(0)\widehat{x}) \qquad \text{on } \widehat{\Gamma},$$

where $\mathbb{J}^{\mathrm{s}}_{\diamond}$ denotes the symmetric part of the Jacobian matrix of $\diamond$, given by $\mathbb{J}^{\mathrm{s}}_{\diamond} = \frac{1}{2}(\mathbb{J}_{\diamond} + \mathbb{J}^{\top}_{\diamond})$. Moreover, the last equation in (A.19) is also a null-charge condition,

$$\int_{\widehat{\Gamma}} \mathbf{n} \cdot \widehat{\boldsymbol{E}}_{1,0}\, ds = -\int_{\widehat{\Gamma}} \underbrace{\mathbf{n} \cdot \widehat{\boldsymbol{E}}_{1,1}}_{=0}\, ds = 0.$$

Then, the unique solutions of (A.19) and (A.20) are given by

$$\begin{aligned} \widehat{\boldsymbol{E}}_{1,0}(\mathrm{X}) &= \frac{1}{\mathrm{R}^4}\left(-\gamma_{\mathrm{t}}\left[\mathbb{J}^{\mathrm{s}}_{\boldsymbol{E}^{\mathrm{i}}}(0)\widehat{x}\right] + \frac{3}{2}\gamma_{\mathrm{n}}\left[\mathbb{J}_{\boldsymbol{E}^{\mathrm{i}}}(0)\widehat{x}\right]\,\widehat{x}\right), && \mathrm{X} \in \widehat{\Omega}, \\ \widehat{\boldsymbol{H}}_{1,0}(\mathrm{X}) &= \frac{1}{\mathrm{R}^4}\left(\frac{2}{3}\gamma_{\mathrm{t}}\left[\mathbb{J}^{\mathrm{s}}_{\boldsymbol{H}^{\mathrm{i}}}(0)\widehat{x}\right] - \gamma_{\mathrm{n}}\left[\mathbb{J}_{\boldsymbol{H}^{\mathrm{i}}}(0)\widehat{x}\right]\,\widehat{x}\right), && \mathrm{X} \in \widehat{\Omega}. \end{aligned} \tag{A.22}$$

From (A.21) and (A.22), we deduce that

$$\widehat{\boldsymbol{E}}_{1,1} = \underset{\mathrm{R}\to\infty}{O}(\mathrm{R}^{-2}), \qquad \widehat{\boldsymbol{H}}_{1,1} = \underset{\mathrm{R}\to\infty}{O}(\mathrm{R}^{-2}) \quad \widehat{\boldsymbol{E}}_{1,0} = \underset{\mathrm{R}\to\infty}{O}(\mathrm{R}^{-4}), \qquad \widehat{\boldsymbol{H}}_{1,0} = \underset{\mathrm{R}\to\infty}{O}(\mathrm{R}^{-4}).$$

Step $p = 2$. Equations *(i)* of (A.14) imply $(\widetilde{\boldsymbol{E}}_2^q, \widetilde{\boldsymbol{E}}_2^q) = (0,0)$ for any $q < 0$. In addition, by *(ii)* of (A.14), we deduce that

$$\widetilde{\boldsymbol{E}}_2 = \widetilde{\boldsymbol{H}}_2 = 0.$$

According to *(iii)*, we deduce that $(\widehat{\boldsymbol{E}}_2^q, \widehat{\boldsymbol{H}}_2^q) = (0,0)$ for any $q \geq 0$. As a consequence,

$$\widehat{\boldsymbol{E}}_2 = \underset{\mathrm{R}\to\infty}{O}(\mathrm{R}^{-1}) \qquad \text{and} \qquad \widehat{\boldsymbol{H}}_2 = \underset{\mathrm{R}\to\infty}{O}(\mathrm{R}^{-1}). \tag{A.23}$$

According to *(iv)-(v)* of (A.14) and (A.23), the second-order terms $\widehat{\boldsymbol{E}}_2$ and $\widehat{\boldsymbol{H}}_2$ solve the following nested Maxwell problems,

$$\begin{cases} \nabla \times \widehat{\boldsymbol{E}}_2 = i\kappa \widehat{\boldsymbol{H}}_1 & \text{in } \widehat{\Omega}, \\ \nabla \cdot \widehat{\boldsymbol{E}}_2 = 0 & \text{in } \widehat{\Omega}, \\ \mathbf{n} \times \widehat{\boldsymbol{E}}_2 = -\dfrac{1}{2}\mathbf{n} \times \left(\widehat{x}^\top \mathbb{H}_{\boldsymbol{E}^i}(0)\widehat{x}\right) & \text{on } \widehat{\Gamma}, \\ \widehat{\boldsymbol{E}}_2 = \underset{\mathrm{R}\to\infty}{O}(\mathrm{R}^{-1}) & \text{at infinity}, \\ \displaystyle\int_{\widehat{\Gamma}} \mathbf{n} \cdot \widehat{\boldsymbol{E}}_2 \, ds = 0, \end{cases} \qquad \begin{cases} \nabla \times \widehat{\boldsymbol{H}}_2 = -i\kappa \widehat{\boldsymbol{E}}_1 & \text{in } \widehat{\Omega}, \\ \nabla \cdot \widehat{\boldsymbol{H}}_2 = 0 & \text{in } \widehat{\Omega}, \\ \mathbf{n} \cdot \widehat{\boldsymbol{H}}_2 = -\dfrac{1}{2}\mathbf{n} \cdot \left(\widehat{x}^\top \mathbb{H}_{\boldsymbol{H}^i}(0)\widehat{x}\right) & \text{on } \widehat{\Gamma}, \\ \widehat{\boldsymbol{H}}_2 = \underset{\mathrm{R}\to\infty}{O}(\mathrm{R}^{-1}) & \text{at infinity}. \end{cases}$$

We decompose the vector fields $\widehat{\boldsymbol{E}}_2$ and $\widehat{\boldsymbol{H}}_2$ under the form

$$\widehat{\boldsymbol{E}}_2 = \widehat{\boldsymbol{E}}_{2,0} + \widehat{\boldsymbol{E}}_{2,1} + \widehat{\boldsymbol{E}}_{2,2} \qquad \text{and} \qquad \widehat{\boldsymbol{H}}_2 = \widehat{\boldsymbol{H}}_{2,0} + \widehat{\boldsymbol{H}}_{2,1} + \widehat{\boldsymbol{H}}_{2,2},$$

where $\widehat{\boldsymbol{E}}_{2,\ell}$ and $\widehat{\boldsymbol{H}}_{2,\ell}$ for $\ell > 0$ are particular solutions of the nested equations obtained by setting $p = 2$ into (A.6),

$$\begin{cases} \nabla \times \widehat{\boldsymbol{E}}_{2,\ell} = i\kappa \widehat{\boldsymbol{H}}_{1,\ell-1} & \text{in } \widehat{\Omega}, \\ \nabla \cdot \widehat{\boldsymbol{E}}_{2,\ell} = 0 & \text{in } \widehat{\Omega}, \\ \widehat{\boldsymbol{E}}_{2,\ell} = \underset{\mathrm{R}\to\infty}{O}(\mathrm{R}^{-1}) & \text{at infinity}, \end{cases} \qquad \begin{cases} \nabla \times \widehat{\boldsymbol{H}}_{2,\ell} = -i\kappa \widehat{\boldsymbol{E}}_{1,\ell-1} & \text{in } \widehat{\Omega}, \\ \nabla \cdot \widehat{\boldsymbol{H}}_{2,\ell} = 0 & \text{in } \widehat{\Omega}, \\ \widehat{\boldsymbol{H}}_{2,\ell} = \underset{\mathrm{R}\to\infty}{O}(\mathrm{R}^{-1}) & \text{at infinity}. \end{cases} \tag{A.24}$$

while $\widehat{\boldsymbol{E}}_{2,0}$ and $\widehat{\boldsymbol{H}}_{2,0}$ solve the static Maxwell problems obtained by taking $p = 2$ and $\ell = 0$ into (A.7) and taking account of the boundary condition (A.5),

$$\begin{cases} \nabla \times \widehat{\boldsymbol{E}}_{2,0} = 0 & \text{in } \widehat{\Omega}, \\ \nabla \cdot \widehat{\boldsymbol{E}}_{2,0} = 0 & \text{in } \widehat{\Omega}, \\ \mathbf{n} \times \widehat{\boldsymbol{E}}_{2,0} = -\mathbf{n} \times \left(\widehat{x}^\top \mathbb{H}_{\boldsymbol{E}^i}(0)\widehat{x}\right) - \mathbf{n} \times \left(\widehat{\boldsymbol{E}}_{2,1} + \widehat{\boldsymbol{E}}_{2,2}\right) & \text{on } \widehat{\Gamma}, \\ \widehat{\boldsymbol{E}}_{2,0} = \underset{\mathrm{R}\to\infty}{O}(\mathrm{R}^{-1}) & \text{at infinity}, \\ \displaystyle\int_{\widehat{\Gamma}} \mathbf{n} \cdot \widehat{\boldsymbol{E}}_{2,0} \, ds = -\int_{\widehat{\Gamma}} \mathbf{n} \cdot \left(\widehat{\boldsymbol{E}}_{2,1} + \widehat{\boldsymbol{E}}_{2,2}\right) ds, \end{cases} \tag{A.25}$$

$$\begin{cases} \nabla \times \widehat{\boldsymbol{H}}_{2,0} = 0 & \text{in } \widehat{\Omega}, \\ \nabla \cdot \widehat{\boldsymbol{H}}_{2,0} = 0 & \text{in } \widehat{\Omega}, \\ \mathbf{n} \cdot \widehat{\boldsymbol{H}}_{2,0} = -\mathbf{n} \cdot \left(\widehat{x}^\top \mathbb{H}_{\boldsymbol{H}^i}(0)\widehat{x}\right) - \mathbf{n} \cdot \left(\widehat{\boldsymbol{H}}_{2,1} + \widehat{\boldsymbol{H}}_{2,2}\right) & \text{on } \widehat{\Gamma}, \\ \widehat{\boldsymbol{H}}_{2,0} = \underset{\mathrm{R}\to\infty}{O}(\mathrm{R}^{-1}) & \text{at infinity}. \end{cases} \tag{A.26}$$

The problems (A.24) for $\ell = 1, 2$, (A.25) and (A.26) are solved with the technique of separation of variables. Particular solutions of (A.24) for $\ell = 1$ are given by

$$\widehat{\boldsymbol{E}}_{2,1}(\mathrm{X}) = \frac{i\kappa}{3\mathrm{R}^3}\gamma_\times\left[\mathbb{J}^{\mathrm{s}}_{\boldsymbol{H}^{\mathrm{i}}}(0)\widehat{x}\right], \qquad \widehat{\boldsymbol{H}}_{2,1}(\mathrm{X}) = \frac{i\kappa}{3\mathrm{R}^3}\gamma_\times\left[\mathbb{J}^{\mathrm{s}}_{\boldsymbol{E}^{\mathrm{i}}}(0)\widehat{x}\right], \qquad \mathrm{X}\in\widehat{\Omega}.$$

Particular solutions of (A.24) for $\ell = 2$ read as

$$\widehat{\boldsymbol{E}}_{2,2}(\mathrm{X}) = \frac{\kappa^2}{2\mathrm{R}}\left(\gamma_{\mathrm{t}}\left[\boldsymbol{E}^{\mathrm{i}}(0)\right] + 2\gamma_{\mathrm{n}}\left[\boldsymbol{E}^{\mathrm{i}}(0)\right]\widehat{x}\right), \qquad \mathrm{X}\in\widehat{\Omega},$$

$$\widehat{\boldsymbol{H}}_{2,2}(\mathrm{X}) = -\frac{\kappa^2}{4\mathrm{R}}\left(\gamma_{\mathrm{t}}\left[\boldsymbol{H}^{\mathrm{i}}(0)\right] + 2\gamma_{\mathrm{n}}\left[\boldsymbol{H}^{\mathrm{i}}(0)\right]\widehat{x}\right), \qquad \mathrm{X}\in\widehat{\Omega}.$$

Note that the *gauge condition* in (A.25) is actually a null-charge condition because $\mathbf{n}\cdot\widehat{\boldsymbol{E}}_{2,1} = 0$ on $\widehat{\Gamma}$ and

$$\int_{\widehat{\Gamma}}\widehat{\boldsymbol{E}}_{2,2}\cdot\mathbf{n} = \kappa^2\int_{\widehat{\Gamma}}\mathbf{n}\cdot\left[\boldsymbol{E}^{\mathrm{i}}(0)\right] = \kappa^2\int_{\mathbb{R}^3\setminus\overline{\widehat{\Omega}}}\nabla\cdot\underbrace{\left[\boldsymbol{E}^{\mathrm{i}}(0)\right]}_{\text{constant}} = 0,$$

where $\mathbb{R}^3\setminus\overline{\widehat{\Omega}}$ is a bounded domain. Hence, the unique solutions of (A.25) and (A.26) are given by

$$\begin{aligned}\widehat{\boldsymbol{E}}_{2,0}(\mathrm{X}) = \frac{1}{\mathrm{R}^5}\Bigg\{ &-\frac{1}{2}\gamma_{\mathrm{t}}\left[\widehat{x}^\top\mathbb{H}_{\boldsymbol{E}^{\mathrm{i}}}(0)\widehat{x}\right] - \frac{i\kappa}{3}\gamma_\times\left[\mathbb{J}^{\mathrm{s}}_{\boldsymbol{H}^{\mathrm{i}}}(0)\widehat{x}\right] - \frac{\kappa^2}{5}\gamma_{\mathrm{t}}\left[\boldsymbol{E}^{\mathrm{i}}(0)\right]\\ &-\frac{4}{3}\bigg(-\frac{1}{2}\gamma_{\mathrm{n}}\left[\widehat{x}^\top\mathbb{H}_{\boldsymbol{E}^{\mathrm{i}}}(0)\widehat{x}\right] - \frac{\kappa^2}{10}\gamma_{\mathrm{n}}\left[\boldsymbol{E}^{\mathrm{i}}(0)\right]\bigg)\widehat{x}\Bigg\} + \frac{3\kappa^2}{10\mathrm{R}^3}\bigg(3\gamma_{\mathrm{n}}\left[\boldsymbol{E}^{\mathrm{i}}(0)\right]\widehat{x} - \boldsymbol{E}^{\mathrm{i}}(0)\bigg),\end{aligned}$$

and

$$\begin{aligned}\widehat{\boldsymbol{H}}_{2,0}(\mathrm{X}) = \frac{1}{\mathrm{R}^5}\Bigg\{ &-\frac{3}{4}\bigg(-\frac{1}{2}\gamma_{\mathrm{t}}\left[\widehat{x}^\top\mathbb{H}_{\boldsymbol{H}^{\mathrm{i}}}(0)\widehat{x}\right] + \frac{i\kappa}{3}\gamma_\times\left[\mathbb{J}^{\mathrm{s}}_{\boldsymbol{E}^{\mathrm{i}}}(0)\widehat{x}\right] - \frac{\kappa^2}{5}\gamma_{\mathrm{t}}\left[\boldsymbol{H}^{\mathrm{i}}(0)\right]\bigg)\\ &-\bigg(\frac{1}{2}\gamma_{\mathrm{n}}\left[\widehat{x}^\top\mathbb{H}_{\boldsymbol{H}^{\mathrm{i}}}(0)\widehat{x}\right] + \frac{\kappa^2}{10}\gamma_{\mathrm{n}}\left[\boldsymbol{H}^{\mathrm{i}}(0)\right]\bigg)\widehat{x}\Bigg\} + \frac{3\kappa^2}{10\mathrm{R}^3}\bigg(3\gamma_{\mathrm{n}}\left[\boldsymbol{H}^{\mathrm{i}}(0)\right]\widehat{x} - \boldsymbol{H}^{\mathrm{i}}(0)\bigg),\end{aligned}$$

for any $\mathrm{X}\in\widehat{\Omega}$.

Step $p = 3$. Equations *(i)* of (A.14) imply

$$(\widetilde{\boldsymbol{E}}_3^{-3}, \widetilde{\boldsymbol{H}}_3^{-3}) = (\widehat{\boldsymbol{E}}_0^{-3}, \widehat{\boldsymbol{H}}_0^{-3}), \qquad (\widetilde{\boldsymbol{E}}_3^{-2}, \widetilde{\boldsymbol{H}}_3^{-2}) = (\widehat{\boldsymbol{E}}_1^{-2}, \widehat{\boldsymbol{H}}_1^{-2}), \quad (\widetilde{\boldsymbol{E}}_3^{-1}, \widetilde{\boldsymbol{H}}_3^{-1}) = (\widehat{\boldsymbol{E}}_2^{-1}, \widehat{\boldsymbol{H}}_2^{-1}). \tag{A.27}$$

Since the outer terms $(\widetilde{\boldsymbol{E}}_3, \widetilde{\boldsymbol{H}}_3)$ are $O(r^{-3})$ when r tends to zero and they satisfy the time-harmonic Maxwell problem *(ii)* of (A.14), we can seek $(\widetilde{\boldsymbol{E}}_3, \widetilde{\boldsymbol{H}}_3)$ under the form

$$\begin{cases}\widetilde{\boldsymbol{E}}_3(x) = h_1^{(1)}(\kappa r)\widetilde{\boldsymbol{u}}_1(\widehat{x}) + \widetilde{h}_1^{(1)}(\kappa r)\widetilde{\boldsymbol{u}}_2(\widehat{x}) + \dfrac{h_1^{(1)}(\kappa r)}{i\kappa r}\widetilde{\boldsymbol{u}}_3(\widehat{x}),\\[2ex] \widetilde{\boldsymbol{H}}_3(x) = h_1^{(1)}(\kappa r)\widetilde{\boldsymbol{v}}_1(\widehat{x}) + \widetilde{h}_1^{(1)}(\kappa r)\widetilde{\boldsymbol{v}}_2(\widehat{x}) + \dfrac{h_1^{(1)}(\kappa r)}{i\kappa r}\widetilde{\boldsymbol{v}}_3(\widehat{x}),\end{cases}$$

see [34, 35]. In the vicinity of the origin, we obtain the following behavior

$$\begin{cases} \widetilde{\boldsymbol{E}}_3(x) = \dfrac{1}{(\kappa r)^3}\left(\widetilde{\boldsymbol{u}}_2 - \widetilde{\boldsymbol{u}}_3\right) - \dfrac{i}{(\kappa r)^2}\widetilde{\boldsymbol{u}}_1 - \dfrac{1}{2\kappa r}\left(\widetilde{\boldsymbol{u}}_2 + \widetilde{\boldsymbol{u}}_3\right) + \underset{r\to 0}{O}(1), \\ \widetilde{\boldsymbol{H}}_3(x) = \dfrac{1}{(\kappa r)^3}\left(\widetilde{\boldsymbol{v}}_2 - \widetilde{\boldsymbol{v}}_3\right) - \dfrac{i}{(\kappa r)^2}\widetilde{\boldsymbol{v}}_1 - \dfrac{1}{2\kappa r}\left(\widetilde{\boldsymbol{v}}_2 + \widetilde{\boldsymbol{v}}_3\right) + \underset{r\to 0}{O}(1). \end{cases} \tag{A.28}$$

Finally, by identifying (A.27) and (A.28) with respect to the (κr)-powers, we obtain

$$\begin{aligned} &\widetilde{\boldsymbol{u}}_1 = -\frac{\kappa^3}{2}\gamma_\times\left[\boldsymbol{H}^{\mathrm{i}}(0)\right], && \widetilde{\boldsymbol{u}}_2 = -\kappa^3\gamma_{\mathrm{t}}\left[\boldsymbol{E}^{\mathrm{i}}(0)\right], && \widetilde{\boldsymbol{u}}_3 = -2\kappa^3\gamma_{\mathrm{n}}\left[\boldsymbol{E}^{\mathrm{i}}(0)\right]\widehat{x}, \\ &\widetilde{\boldsymbol{v}}_1 = -\kappa^3\gamma_\times\left[\boldsymbol{E}^{\mathrm{i}}(0)\right], && \widetilde{\boldsymbol{v}}_2 = \frac{\kappa^3}{2}\gamma_{\mathrm{t}}\left[\boldsymbol{H}^{\mathrm{i}}(0)\right], && \widetilde{\boldsymbol{v}}_3 = \kappa^3\gamma_{\mathrm{n}}\left[\boldsymbol{H}^{\mathrm{i}}(0)\right]\widehat{x}. \end{aligned}$$

Remark 9. Actually, only the knowledge of $\widetilde{\boldsymbol{u}}_1$ and $\widetilde{\boldsymbol{v}}_1$ is needed to compute the third-order outer terms $(\widetilde{\boldsymbol{E}}_3, \widetilde{\boldsymbol{H}}_3)$. Indeed, properties of duality for outgoing solutions of time-harmonic Maxwell equations imply that

$$\widetilde{\boldsymbol{v}}_2 = \widehat{x} \times \widetilde{\boldsymbol{u}}_1 \qquad \text{and} \qquad \widetilde{\boldsymbol{u}}_2 = \widetilde{\boldsymbol{v}}_1 \times \widehat{x}.$$

Moreover, the last unknown vectors $\widetilde{\boldsymbol{u}}_3$ and $\widetilde{\boldsymbol{v}}_3$ can be deduced from the identification with respect to $(\kappa r)^{-3}$ of(A.27) with (A.28). As a consequence, the computation of $(\widetilde{\boldsymbol{E}}_4, \widetilde{\boldsymbol{H}}_4)$ is reduced to 4 unknown vector fields, the computation of $(\widetilde{\boldsymbol{E}}_5, \widetilde{\boldsymbol{H}}_5)$ is reduced to 6 unknown vectors fields and so on. In particular, the outer terms $(\widetilde{\boldsymbol{E}}_4, \widetilde{\boldsymbol{H}}_4)$ are entirely determined by the conditions extracted from *(i)* of (A.14), given by

$$(\widetilde{\boldsymbol{E}}_4^{-3}, \widetilde{\boldsymbol{H}}_4^{-3}) = (\widehat{\boldsymbol{E}}_1^{-3}, \widehat{\boldsymbol{H}}_1^{-3}) = (0,0) \qquad \text{and} \qquad (\widetilde{\boldsymbol{E}}_4^{-4}, \widetilde{\boldsymbol{H}}_4^{-4}) = (\widehat{\boldsymbol{E}}_0^{-4}, \widehat{\boldsymbol{H}}_0^{-4}) = (0,0).$$

As a result, $(\widetilde{\boldsymbol{E}}_4, \widetilde{\boldsymbol{H}}_4) = (0,0)$. Likewise, the outer terms $(\widetilde{\boldsymbol{E}}_5, \widetilde{\boldsymbol{H}}_5)$ are entirely determined by the conditions extracted from *(i)* of (A.14), given by

$$\begin{cases} (\widetilde{\boldsymbol{E}}_5^{-3}, \widetilde{\boldsymbol{H}}_5^{-3}) = (\widehat{\boldsymbol{E}}_2^{-3}, \widehat{\boldsymbol{H}}_2^{-3}) \neq (0,0), \\ (\widetilde{\boldsymbol{E}}_5^{-4}, \widetilde{\boldsymbol{H}}_5^{-4}) = (\widehat{\boldsymbol{E}}_1^{-4}, \widehat{\boldsymbol{H}}_1^{-4}) \neq (0,0), \\ (\widetilde{\boldsymbol{E}}_5^{-5}, \widetilde{\boldsymbol{H}}_5^{-5}) = (\widehat{\boldsymbol{E}}_0^{-5}, \widehat{\boldsymbol{H}}_0^{-5}) = (0,0). \end{cases}$$

Appendix A.6. Error estimates

For any non-negative integer $P \in \mathbb{N}$, we introduce the vector fields $\widetilde{\boldsymbol{E}}_{\delta,P}$ and $\widetilde{\boldsymbol{H}}_{\delta,P}$, respectively $\widehat{\boldsymbol{E}}_{\delta,P}$ and $\widehat{\boldsymbol{H}}_{\delta,P}$, reading as the truncated series made up of the $P+1$ first terms of the outer expansion, respectively of the inner expansion,

$$\widetilde{\boldsymbol{E}}_{\delta,P}(x) = \sum_{p=0}^{P} \delta^p \widetilde{\boldsymbol{E}}_p(x), \qquad \widetilde{\boldsymbol{H}}_{\delta,P}(x) = \sum_{p=0}^{P} \delta^p \widetilde{\boldsymbol{H}}_p(x), \qquad x \in \Omega^\star, \tag{A.29}$$

$$\widehat{\boldsymbol{E}}_{\delta,P}(\mathrm{X}) = \sum_{p=0}^{P} \delta^p \widehat{\boldsymbol{E}}_p(\mathrm{X}), \qquad \widehat{\boldsymbol{H}}_{\delta,P}(\mathrm{X}) = \sum_{p=0}^{P} \delta^p \widehat{\boldsymbol{H}}_p(\mathrm{X}) \qquad \mathrm{X} \in \widehat{\Omega}. \tag{A.30}$$

In a further work, we will prove that the local approximations of solution to problem (2.1) are subject to the following error estimates. There exists a positive δ_0 such that for any $r_1 > r_0 > \delta_0$ there exists $c > 0$ such that for any positive $\delta < \delta_0$, we have

$$\|\boldsymbol{E}_\delta - \widetilde{\boldsymbol{E}}_{\delta,P}\|_{\mathrm{L}^2(\mathcal{C}(r_0,r_1))} \leq c\,\delta^{P+1}, \qquad \|\boldsymbol{H}_\delta - \widetilde{\boldsymbol{H}}_{\delta,P}\|_{\mathrm{L}^2(\mathcal{C}(r_0,r_1))} \leq c\,\delta^{P+1}. \tag{A.31}$$

There exists $\mathrm{R}^\star > \delta_0$ such that for any R_0 satisfying $1 < \mathrm{R}_0 < \mathrm{R}^\star$, there exists $c > 0$ such that for any positive $\delta < \delta_0$, we have

$$\|\boldsymbol{E}_\delta(\delta\,\cdot\,) - \widehat{\boldsymbol{E}}_{\delta,P}\|_{\mathrm{L}^2(\mathcal{C}(1,\mathrm{R}_0))} \leq c\,\delta^{P+\frac{5}{2}}, \qquad \|\boldsymbol{H}_\delta(\delta\,\cdot\,) - \widehat{\boldsymbol{H}}_{\delta,P}\|_{\mathrm{L}^2(\mathcal{C}(1,\mathrm{R}_0))} \leq c\,\delta^{P+\frac{5}{2}}. \tag{A.32}$$

Remark 10. In [28], Ammari *et al.* showed that estimate (A.32) holds for $P = 0$. In [19], the authors used the method of multi-scale expansions to define an approximate solution of the electromagnetic scattering problem by a small obstacle and proved error estimates for the asymptotics at any order. They set up a rigorous framework to make the asymptotic analysis of the time-harmonic Maxwell problem including elliptic regularization and the time-dependent Maxwell problem. Moreover, they consider either a condition of perfect conductor or an impedance condition. Regarding of [18] and [33, Appendix C.2], we can state that the expansions provided by the method of matched asymptotic expansions and the method of multi-scale expansions locally coincide. As a result, error estimates from [19] hold for the matched asymptotic expansions. However, the authors adopt a slightly different framework: the wave number κ has a positive imaginary part and the domain of propagation Ω_δ is bounded with smooth boundary. It seems possible not only to adapt and generalize these estimates by considering a more general framework, but also to improve their non-optimal estimates.

References

[1] J. Blitz, Electrical and magnetic methods of non-destructive testing, volume 3, Springer Science & Business Media, 2012.

[2] K. A. Fuller, D. W. Mackowski, Electromagnetic scattering by compounded spherical particles, Light scattering by nonspherical particles: theory, measurements, and applications (2000) 226.

[3] B. Veihelmann, T. Nousiainen, M. Kahnert, W. Van der Zande, Light scattering by small feldspar particles simulated using the gaussian random sphere geometry, Journal of Quantitative Spectroscopy and Radiative Transfer 100 (2006) 393–405.

[4] T. Wriedt, J. Hellmers, E. Eremina, R. Schuh, Light scattering by single erythrocyte: comparison of different methods, Journal of Quantitative Spectroscopy and Radiative Transfer 100 (2006) 444–456.

[5] A. G. Ramm, Scattering by Obstacles, Springer, 1986.

[6] A. G. Ramm, Wave scattering by small bodies of arbitrary shapes, Springer, 2005.

[7] P. A. Martin, Multiple scattering: interaction of time-harmonic waves with N obstacles, 107, Cambridge University Press, 2006.

[8] H. Ammari, H. Kang, H. Lee, M. Lim, S. Yu, Enhancement of near cloaking for the full maxwell equations, SIAM Journal on Applied Mathematics 73 (2013) 2055–2076.

[9] M. Ganesh, S. C. Hawkins, A high-order algorithm for multiple electromagnetic scattering in three dimensions, Numerical Algorithms 50 (2009) 469–510.

[10] B. Thierry, Analyse et simulations numériques du retournement temporel et de la diffraction multiple, Ph.D. thesis, 2011.

[11] H. Barucq, J. Chabassier, H. Pham, S. Tordeux, Numerical robustness of single-layer method with Fourier basis for multiple obstacle acoustic scattering in homogeneous media, Wave Motion (2017).

[12] D. G. Crighton, A. P. Dowling, J. Ffowcs-Williams, M. Heckl, F. Leppington, J. F. Bartram, Modern methods in analytical acoustics lecture notes, 1992.

[13] W. Eckhaus, Matched asymptotic expansions and singular perturbations (1973).

[14] A. M. Il'in, Matching of asymptotic expansions of solutions of boundary value problems, volume 102, American Mathematical Society Providence, RI, 1992.

[15] V. Maz'Ya, S. Nazarov, B. Plamenevskij, Asymptotic theory of elliptic boundary value problems in singularly perturbed domains, volume 1, Birkhäuser, 2012.
[16] V. Bonnaillie-Noël, D. Brancherie, M. Dambrine, F. Herau, S. Tordeux, G. Vial, Multiscale expansion and numerical approximation for surface defects, in: ESAIM: Proceedings, volume 33, EDP Sciences, 2011, pp. 22–35.
[17] P.-H. Cocquet, Étude mathématique et numérique de modéles homogénéisés de métamatériaux, Ph.D. thesis, Université Paul Sabatier-Toulouse III, 2012.
[18] M. Dauge, S. Tordeux, G. Vial, Selfsimilar perturbation near a corner: matching versus multiscale expansions for a model problem, in: Around the Research of Vladimir Maz'ya II, Springer, 2010, pp. 95–134.
[19] D. Korikov, B. A. Plamenevskii, Asymptotics of solutions for stationary and nonstationary maxwell systems in a domain with small holes, Algebra i Analiz 28 (2016) 102–170.
[20] X. Claeys, Analyse asymptotique et numérique de la diffraction d'ondes par des fils minces, Ph.D. thesis, Université de Versailles-Saint Quentin en Yvelines, 2008.
[21] V. Mattesi, Propagation des ondes dans un domaine comportant des petites hétérogénéités: modélisation asymptotique et calcul numérique, Ph.D. thesis, Pau, 2014.
[22] M. Van Dyke, Perturbation Methods in Fluid Mechanics, Parabolic Press, 1975.
[23] A. Bendali, P.-H. Cocquet, S. Tordeux, Approximation by multipoles of the multiple acoustic scattering by small obstacles in three dimensions and application to the foldy theory of isotropic scattering, Archive for Rational Mechanics and Analysis 219 (2016) 1017–1059.
[24] A. Bouzekri, M. Sini, The foldy–lax approximation for the full electromagnetic scattering by small conductive bodies of arbitrary shapes, Multiscale Modeling & Simulation 17 (2019) 344–398.
[25] D. P. Challa, G. Hu, M. Sini, Multiple scattering of electromagnetic waves by finitely many point-like obstacles, Mathematical Models and Methods in Applied Sciences 24 (2014) 863–899.
[26] L. L. Foldy, The multiple scattering of waves. I. General theory of isotropic scattering by randomly distributed scatterers, Physical Review 67 (1945) 107.
[27] H. Ammari, A. Khelifi, Electromagnetic scattering by small dielectric inhomogeneities, Journal de mathématiques pures et appliquées 82 (2003) 749–842.
[28] H. Ammari, M. S. Vogelius, D. Volkov, Asymptotic formulas for perturbations in the electromagnetic fields due to the presence of inhomogeneities of small diameter II: The full Maxwell equations, Journal de mathématiques pures et appliquées 80 (2001) 769–814.
[29] H. Ammari, S. Moskow, M. S. Vogelius, Boundary integral formulae for the reconstruction of electric and electromagnetic inhomogeneities of small volume, ESAIM: Control, Optimisation and Calculus of Variations 9 (2003) 49–66.
[30] H. Ammari, H. Kang, Reconstruction of small inhomogeneities from boundary measurements, Springer, 2004.
[31] H. Ammari, H. Kang, Polarization and moment tensors: with applications to inverse problems and effective medium theory, volume 162, Springer Science & Business Media, 2007.
[32] C. F. Bohren, D. R. Huffman, Absorption and scattering of light by small particles, John Wiley & Sons, 2008.
[33] J. Labat, V. Péron, S. Tordeux, Asymptotic modeling of the electromagnetic scattering by small spheres perfectly conducting, Research Report RR-9169, 2018. URL: `https://hal.inria.fr/hal-01762625`.
[34] P. Monk, Finite element methods for Maxwell's equations, Oxford University Press, 2003.
[35] J.-C. Nédélec, Acoustic and electromagnetic equations: integral representations for harmonic problems, volume 144, Springer Science & Business Media, 2001.
[36] J. Labat, Représentations modales pour la diffraction d'ondes électromagnétiques, Master's thesis, Université de Pau et des Pays de l'Adour, 2016. URL: `https://hal.inria.fr/hal-01726506`.
[37] B. G. Korenev, Bessel functions and their applications, CRC Press, 2003.
[38] J. D. Jackson, Classical electrodynamics, 3rd ed., Wiley, 1999.
[39] B. Laud, Electromagnetics, New Age International, 1987.
[40] M. Born, E. Wolf, Principles of optics: electromagnetic theory of propagation, interference and diffraction of light, Elsevier, 2013.
[41] H. Kogelnik, T. Li, Laser beams and resonators, Applied optics 5 (1966) 1550–1567.
[42] Y.-L. Xu, Electromagnetic scattering by an aggregate of spheres, Applied optics 34 (1995) 4573–4588.
[43] A. Egel, L. Pattelli, G. Mazzamuto, D. S. Wiersma, U. Lemmer, Celes: Cuda-accelerated simulation of electromagnetic scattering by large ensembles of spheres, Journal of Quantitative Spectroscopy and Radiative Transfer 199 (2017) 103–110.
[44] M. Costabel, M. Dauge, S. Nicaise, Singularities of eddy current problems, ESAIM: Mathematical Modelling and Numerical Analysis 37 (2003) 807–831.
[45] R. Hiptmair, Symmetric coupling for eddy current problems, SIAM Journal on Numerical Analysis 40 (2002) 41–65.
[46] V. Péron, Asymptotic models and impedance conditions for highly conductive sheets in the time-harmonic eddy current models, SIAM Journal on Applied Mathematics (2019). Accepted.